GLYCATED BOVINE SERUM ALBUMIN FOR CURCUMIN NANOENCAPSULATION: BIO-NANO INTERACTIONS

RENATA PFEILSTICKER NEVES

Thesis submitted to the University of Ottawa
in partial fulfillment of the requirements for the
Master's degree in Chemistry

Department Chemistry and Biomolecular Sciences
Faculty of Science
University of Ottawa

À Debora, Onelia e Lola

Table of Contents

List of Figures

List of Tables

List of Abbreviations

BSA	Bovine serum albumin
DG	Degree of glycation
DLS	Dynamic light scattering
FITC-WGA	FITC labeled wheat germ agglutinin
GIT	Gastrointestinal tract
HSA	Human serum albumin
Lys	Lysine
MW	Molecular weight
NP	Nanoparticle
PBS	Phosphate buffered saline
PBST	Phosphate buffered saline containing 0.05% Tween 20
PDI	Polydispersity index
pI	Isoelectric point
RES	Reticuloendothelial system
SA	Serum albumin
SDS-PAGE	Sodium dodecyl sulphate–polyacrylamide gel electrophoresis
Trp	Tryptophan
WP	Whey protein

Abstract

Glycation of whey proteins results in food-grade composites with modified physicochemical properties. Here, the reaction between glucose and bovine serum albumin (BSA) is promoted under wet-heating conditions. The glycated protein is characterized in depth and compared to the native counterpart and the impact of glycation on properties like net surface charge, particle size and surface hydrophobicity are observed. Conjugation with glucose reduced the surface hydrophobicity of BSA but the interactions between albumin and curcumin became stronger, which contradicts the direct relationship between curcumin binding affinity and protein surface hydrophobicity described in the literature. Nonetheless, curcumin was still capable of quenching the intrinsic fluorescence of the protein after conjugation with glucose and leads to the conclusion that curcumin and BSA interact in a different manner upon glycation. This thesis also depicts mucin as a forthcoming model in the study of nanoparticle interactions with intestinal mucus and glycation posed no effect on such interactions.

Keywords: Glycation, whey proteins, curcumin, nanocarrier, nano-bio interactions.

Acknowledgements

I would like to express my deepest gratitude to my research supervisors Dr. Udenigwe and Dr. Musgaard for the opportunity to pursue my graduate studies at uOttawa, and to MITACS for opening this door for me in 2019. Thank you Dr. Avis and Dr. Blais for kindly accepting my invitation be in the TAC and for taking the time to read my thesis.

I would like to share my love and appreciation to everyone in the Udenigwe Lab (2019 – 2021). You are amazing people and I can't wait to see what you achieve next.

I would like to say thanks to Dr. Udenigwe for the extraordinary leadership. You motivated me without even knowing it and showed me what a true leader is all about. You are an inspiration to me personally and professionally. I am grateful for the financial support and for your guidance in my path to stay in Canada. Thank you for pushing me to be the best researcher I can be, I appreciate it. But most of all, thank you for believing in me and welcoming me into your group.

I wanted to say a special thank you to Xiaohong and Ogadimma for the countless times you have helped me. I learned so much from you and would not be able to achieve this without you. I am grateful for your kindness, guidance, feedback, friendship and mentorship throughout this project. You both made long experiments an enjoyable experience and I will miss you dearly.

Thank you to all my friends in Bauru, Vitoria and Ottawa for the love and encouragement. A special thank you goes to Raliat and Salmaan. I love you both and your friendship means the world to me. Thank you for always being there for me and making the past year and a half so memorable.

Finally, I want to thank my mom, my (step)dad and Blair for their unconditional love and support. Your calls at inconvenient times, heartfelt pep talks and encouragement kept me motivated through the pandemic and you are the reason I work so hard. Eu amo vocês.

Chapter 1

Introduction

1.1 Whey protein

Whey is a secondary protein group in bovine milk with a protein content <1% (E. A. Foegeding et al., 2002), while casein is the main group and corresponds to 70 - 80% of total protein content in milk (Khezri S., Seyedsaleh M.M., Seyedsaleh I., Dastras M., Dehghan P., 2016). Consequently, whey used to be known as the liquid waste of dairy manufacturing, matching around 90% of the milk discarded during the production of cheese (Khezri S., Seyedsaleh M.M., Seyedsaleh I., Dastras M., Dehghan P., 2016).

Though the protein content is modest, whey is no longer a mere waste of the milk industry and is now considered a rich mixture of globular proteins hence the name whey proteins. Its popularity ascended fast as whey proteins became a high-demand staple for supplements (Hoffman & Falvo, 2004), food packaging, animal feed and fertilizers (Khezri S., Seyedsaleh M.M., Seyedsaleh I., Dastras M., Dehghan P., 2016). Shortly, other uses beyond the food industry were established. For instance, in the production of adhesives (Guo & Wang, 2016), treatment of chronic diseases, and for the delivery of biologically active compounds (Gunasekaran et al., 2007; Hoffman & Falvo, 2004; Marshall, 2004; Murthy et al., 2018; Sanidad et al., 2019).

Whey protein (WP) is generally commercialized as a dried powder that is soluble at pH 4.6 (20°C) (Farooq et al., 2019; Farrell et al., 2004; Lohcharoenkal et al., 2014; Ramos et al., 2019). In 1972, whey powder was the most common form of processed whey for both animal and human nutrition, followed by each WP fraction individually (Delaney et al., 1972). The main protein fractions in WP can be seen in Figure 1.1. Because of its diverse composition, WP contains a broad

variety of essential and branched-chain amino acids, bioactive peptides, immunopotentiators and antioxidants (Hoffman & Falvo, 2004; Patel, 2015).

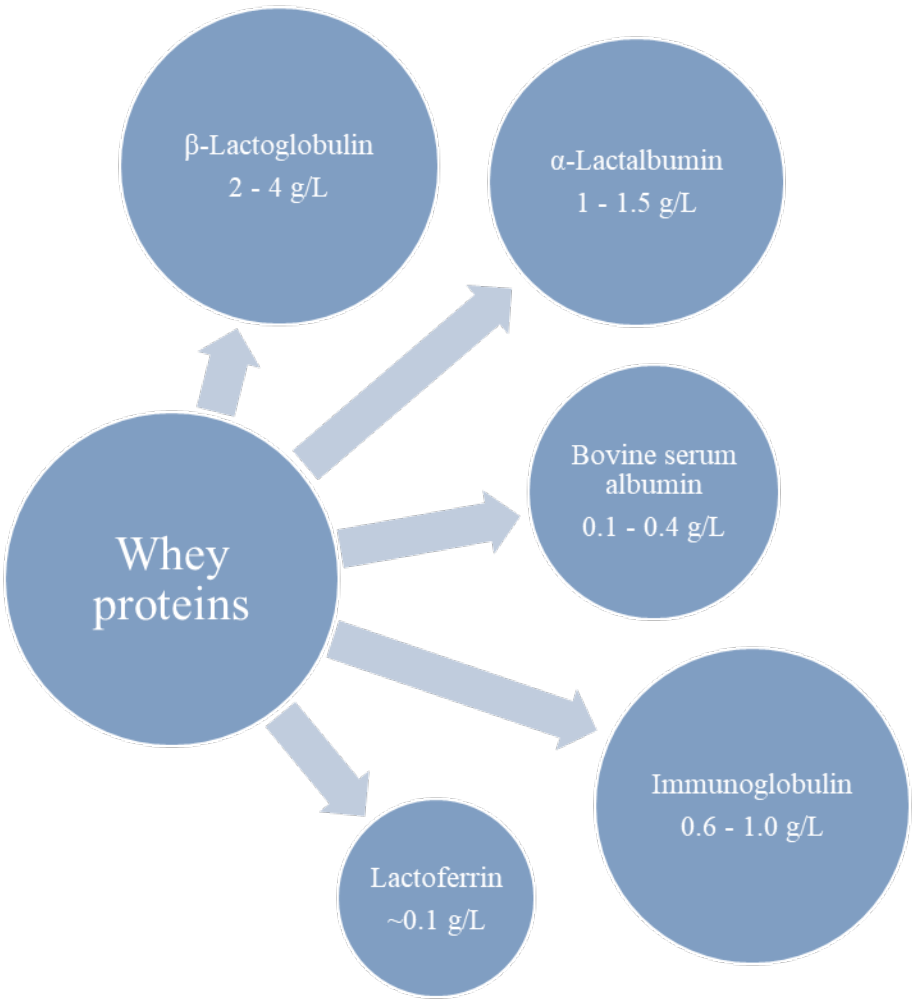

Figure 1.1 Protein composition of whey

Concentration of each whey protein fraction corresponds to their respective content in bovine milk (Livney, 2010).

Protein content is the most used parameter in WP categorization, for which there are two main classifications: concentrate (WPC, 20 - 89% protein) and isolate (WPI, ≥ 90% protein) (E.

A. Foegeding et al., 2002; E. Foegeding & Luck, 2002; Guo & Wang, 2016; Hoffman & Falvo, 2004; Tunick, 2008). To achieve high protein concentrations, filtration methods can be applied either alone or combined, and are usually followed by a drying step (E. Foegeding & Luck, 2002; Tunick, 2008). WP processing is relevant for certain applications because there is a dependent relationship between processing enforcement, protein integrity and bioactivity. Over-purification of whey induces protein denaturation and/or breakage (Hoffman & Falvo, 2004) and some natural-occurring functional properties of WPs are reduced upon heat denaturation (Delaney et al., 1972).

Many studies on whey applications are directed to functional foods and/or to drug encapsulation and delivery due to WP's great foaming, gelling and emulsifying properties (Arroyo-Maya et al., 2012; Fan et al., 2017; Jayaprakasha et al., 2016; Lohcharoenkal et al., 2014; Mehravar et al., 2009; Pan, Li, et al., 2020; Taghavi Kevij et al., 2019). Not only are milk-derived proteins one of the lowest cost protein sources (Pellegrino et al., 2013), but WPs are also a suitable alternative to synthetic polymers as nanocarriers (Jayaprakasha et al., 2016). Moreover, WP's amphiphilicity, excellent nutritional value and abundance make it a very convenient material for nanoencapsulation (Arroyo-Maya et al., 2012; Mehravar et al., 2009; Taghavi Kevij et al., 2019).

WPs can be synthesized as nanoparticles or nanoemulsions and are efficient in encapsulating hydrophilic and hydrophobic molecules. During synthesis, an easy manipulation of conditions (e.g. pH, temperature and ionic strength) directs the particle size to fall within the nano range (Mohammadian et al., 2019). WP nanoparticles are biodegradable, can be chemically modified, offer great binding capacity and can be metabolized by the body (Jahanshahi & Babaei, 2008).

1.2 Bovine serum albumin

Albumin is obtained from different sources like eggs (ovalbumin), cow's milk and meat (bovine serum albumin, BSA) and rice bran (rice bran albumin), as well as from the plasma of a variety of animals such as horse, rabbit, cattle and humans (Elzoghby et al., 2012; Lohcharoenkal et al., 2014; Majorek et al., 2012; H. Peng et al., 2017).

Serum albumin (SA) is indispensable for the maintenance of biological conditions in mammals. It facilitates osmotic pressure regulation (Lohcharoenkal et al., 2014) and transports endo- and exogenous substances. SA is a natural transporter of nutrients and metabolites in the plasma of mammals because of the high amount of open binding sites that it contains, hence SA being the most abundant protein in the plasma of many species (Majorek et al., 2012; Ullrey, 2009a, 2009b).

There are approximately 60 mg of human serum albumin (HSA) per 100 mL of breast milk (Bezkorovainy, 1977). Comparatively, BSA's overall concentration in milk is relatively low (40 mg/100 mL bovine milk), but it represents the third most abundant protein in whey: around 10% of total protein content (Farrell et al., 2004; Marshall, 2004). Human and bovine serum albumin are commonly used for pharma- and nutraceutical research and applications because of their structural and functional similarities. Residue sequences of HSA and BSA have around 80% similarity and it has been reported that nearly all of their physical aspects are identical (Peters, 1985).

BSA is a large, heart-shaped, amphiphilic protein with high water solubility and negative charge at pH 7 (Carter & Ho, 1994; Majorek et al., 2012). BSA has a molecular weight of approximately 66.0 kDa (Fan et al., 2017) and its globular structure contains numerous binding sites, reactive functional groups (e.g., amino, carboxyl and thiol) and essential amino acids

(Lohcharoenkal et al., 2014; Majorek et al., 2012; Marshall, 2004). Each molecule, as most serum albumins, is divided into domains I, II and III and their respective subdomains A and B (Farrell et al., 2004; O'Mahony & Fox, 2013). Although BSA has only one sulfhydryl group, it presents 17 disulfides that can bind BSA intermolecularly to α-lactalbumin and β-lactoglobulin through the induction of heat (Carter & Ho, 1994; Farrell et al., 2004; O'Mahony & Fox, 2013). Besides being flexible, the structure of BSA remains stable in a wide pH range (from 4 to 9) and does not show evidence of degradation or damage in temperatures up to 60°C (Lohcharoenkal et al., 2014). Peters (1985) pointed out that while some conditions are damaging to other proteins (i.e., long exposure to temperatures > 50°C), BSA withstands the same conditions without damage and can return to its native conformation afterwards.

1.3 Curcumin as a hydrophobic bioactive molecule

Curcumin is a natural polyphenol found in turmeric (*Curcuma* species) (Cas & Ghidoni, 2019). Its structure is illustrated in Figure 1.2 and suffers keto-enol tautomerism depending on the pH (not shown) (Anand et al., 2007). Recently, curcumin has been extensively researched because of its outstanding health enhancing and pharmacological potential that includes, but is not limited to, anti-inflammatory, anti-allergic, antidiabetic and anti-cancer applications (Cas & Ghidoni, 2019; Sanidad et al., 2019).

Most pharmacological properties of curcumin are closely dependant on the structure of the molecule but finding conditions in which curcumin is stable has been a challenge for researchers. Curcumin oxidizes itself in physiological conditions (neutral pH) leading to a half-life of 1 - 9 minutes (Sanidad et al., 2019) and in basic pH the molecular structure undergoes cleavage (Cas &

Ghidoni, 2019). Curcumin is extremely insoluble in water at acidic pH but chemically stable. Lastly, curcumin is also light sensitive and suffers light-induced oxidation (Cas & Ghidoni, 2019).

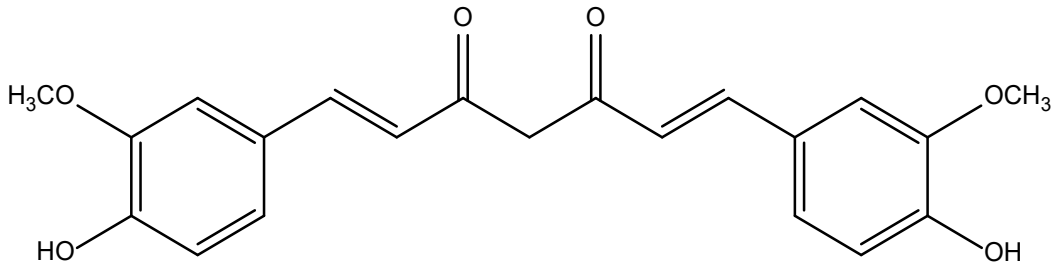

Figure 1.2 Chemical structure of curcumin.

The poor solubility and instability of curcumin in physiological conditions impacts its absorption kinetics negatively, meaning that curcumin's health-enhancing effects are not fully exploited after consumption (Liang et al., 2008). Anand et al. (2007) compiled the findings of many studies on tissue and plasma distribution of curcumin after oral, intravenous and intraperitoneal administration, but curcumin presented an overall quick elimination from the body and low absorption.

Nanoencapsulation is a great strategy to overcome the very limited bioavailability of curcumin by enhancing its solubility and facilitating absorption (Cas & Ghidoni, 2019). Moreover, nanocarriers provide a protective layer that isolates curcumin from pH and light induced modifications. Many strategies for encapsulation of curcumin were investigated and described in the literature, but food-grade delivery systems stand out for their safety and likely use in functionalized foods and beverages (Rafiee et al., 2019; Sanidad et al., 2019). Table 1.1 describes a few examples of food-grade WP-based nanocarriers tested for the encapsulation and delivery of curcumin.

Table 1.1 Examples of whey protein-based nanodelivery systems tested for the encapsulation of curcumin.

WP-based nanocarrier	Reference
BSA	(Salehiabar et al., 2018)
BSA, dextran	(Fan et al., 2018)
BSA, iron oxide	(Nosrati et al., 2018)
WP	(Jayaprakasha et al., 2016; Pan, Li, et al., 2020; Taghavi Kevij et al., 2019)
α-Lactalbumin, dextran	(Yi et al., 2016)
β-Lactoglobulin	(Kanakis et al., 2013; Sneharani et al., 2010; Teng et al., 2014)
β-Lactoglobulin, sodium alginate	(Hosseini et al., 2015)

1.4 BSA in curcumin nanoencapsulation

BSA has many attributes that make it a suitable material for nanodelivery industry and research such as low-cost, ease of purification, biodegradability, and biocompatibility (Elzoghby et al., 2012; Kratz, 2008; Nosrati et al., 2018; Pellegrino et al., 2013). The remarkable functionality and safety of BSA are the main reason behind the long-standing support of biomedical research towards the use of BSA in drug design and contrast imaging techniques. Namely, BSA has an excellent ligand-binding capacity, besides being nontoxic and less prone to induce allergic reactions than α-lactalbumin, β-lactoglobulin or casein (Caira et al., 2012; Carter & Ho, 1994; Jahanshahi & Babaei, 2008).

As for nanoencapsulation and delivery of curcumin, BSA can modify its conformation to accommodate ligands without losing stability (Peters, 1985) and has affinity towards hydrophobic and hydrophilic compounds (Lohcharoenkal et al., 2014). So, while curcumin is entrapped in a hydrophobic core of the nanoparticle, the hydrophilic surface promotes solubility of the carrier. Additional to hydrophobic interactions with BSA, curcumin has keto, OH and methoxy groups

that can form hydrogen bonds with the protein. Covalent binding of ligands to albumin NPs has also been reported before (Jahanshahi & Babaei, 2008).

Albumin NPs show superior uptake by solid tumors compared to other carriers, specially if their size is around 200 nm (Jithan et al., 2011; Kratz, 2008; Lohcharoenkal et al., 2014; Noguchi et al., 1998). Additionally, NPs of ~100 nm tend to escape the vascular system thus reaching other tissues with ease through passive tissue targeting (Jithan et al., 2011; Kratz, 2008; Noguchi et al., 1998; Wu et al., 1997). This is particularly beneficial to nanoencapsulation because it hinders recognition by opsonins, leading to difficulties in the elimination of carriers by the reticuloendothelial system (RES). Noguchi (1998) demonstrated that molecules of higher molecular weight (≥ 40 kDa) accumulate in solid tumors with time, whereas low molecular weight particles (< 20 kDa) reverse back into the blood and are rapidly excreted. Then, the large size and molecular weight of BSA (~66 kDa) is optimal for targeted delivery of curcumin, and its enhanced tissue permeability can be used as an asset in anti-cancer and anti-inflammatory applications.

1.5 Protein glycation for improving functionality

Nanoencapsulation is only truly effective if the carrier is able to reach the delivery site intact and then slowly release the bioactive compound (Cas & Ghidoni, 2019). Many authors consider and use chemical modification as an approach to improve NP stability (Davidov-Pardo et al., 2015; Gunasekaran et al., 2007; Wang et al., 2008; Yi et al., 2014). The surface of BSA NPs has amino, carboxylic and thiol groups that can be used for chemical modification (Jahanshahi & Babaei, 2008).

The Maillard reaction, also known as glycation, is a noteworthy example of food-grade approach to NP surface modification through the spontaneous reaction of proteins and reducing

sugars. It occurs naturally in foods during long term storage and is stimulated by heat during cooking (Chevalier, Chobert, Genot, et al., 2001; Livney, 2010). Chemically, glycation happens between ε-amino groups of the protein and reducing end of sugar molecules (carbonyl group) (Figure 1.3). In BSA, exposed lysine residues are largely responsible for providing the amino groups necessary for the reaction. Lysine has two amino groups thus providing more binding sites for sugar molecules than other BSA residues (Kato, 2002).

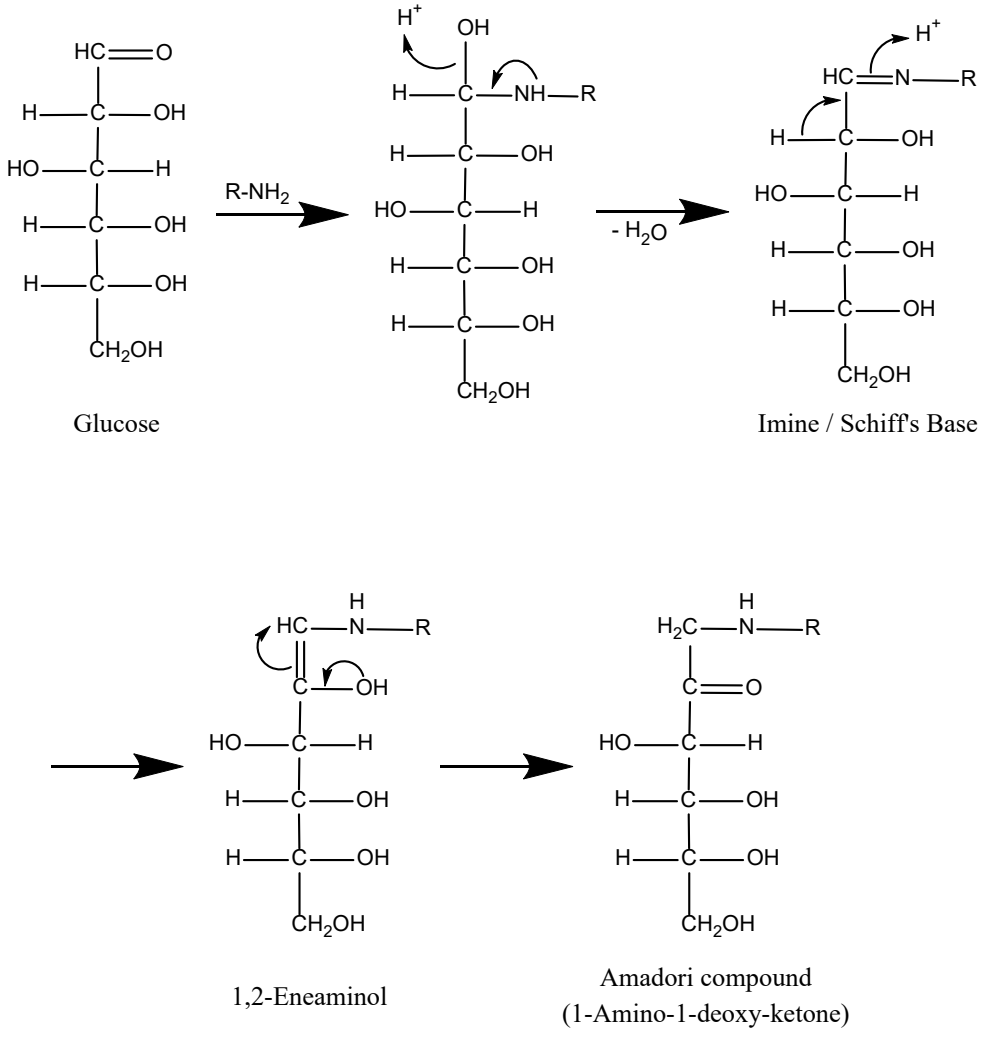

Figure 1.3 Schematic representation of glucose binding to BSA.

The scheme shows the early stage of the Maillard reaction.

Glycation is a very complex reaction with three stages: initial, advanced and final. The point of interest for protein NP modification is the initial stage. Advanced glycation end products (AGEs) are formed in the last two stages of the reaction and have been linked to the development and worsening of many health complications, e.g. diabetes (Lin et al., 2018; Singh et al., 2014). Fortunately, the extent of Maillard reaction can be controlled through different time-temperature combinations amongst other factors (Lund & Ray, 2017; Zhang et al., 2019).

Different approaches can be taken to glycate proteins, and the main methods are dry-heating and wet-heating (Zhang et al., 2019). The first is the heating of protein and sugar in the solid state and the reaction is easily controlled if the temperature used is higher than 60℃, but high temperatures lead to protein denaturation and loss of bioactivity. On the other hand, lower temperatures can be used in wet-heating. This method uses water as the reaction media, subsequently shifting the equilibrium towards the reagents, since water is one of the products of glycation (Figure 1.3). Equilibrium shift is an advantage because the reaction is slowed down and can easily be stopped before the advanced and final stages of the Maillard reaction, thus avoiding formation of AGEs.

Glycation has been proven effective in many whey proteins for the encapsulation of drugs and nutraceuticals, including curcumin and β-carotene (Chevalier, Chobert, Genot, et al., 2001; Fan et al., 2017, 2018; Jung et al., 2006; Ledesma-Osuna et al., 2008; Yi et al., 2014). Glycation of BSA improves heat and digestion stability, as well as other physicochemical properties like texture and gelling ability (Kato, 2002; G. Liu & Zhong, 2012; Lund & Ray, 2017; Morgan et al., 1999; Tsekovska et al., 2016). Enhancing digestion stability of BSA is particularly interesting for delivery of curcumin, because it would mean that curcumin is protected throughout the gastrointestinal tract (GIT) and then the released would happen slowly in the intestine. Over the

years BSA has been glycated with many carbohydrates including glucose, lactose and galactose (Ledesma-Osuna et al., 2008; J. Liu & Jing, 2016; Rondeau et al., 2010), as well as dextran (Fan et al., 2018; Hao et al., 2014; Jung et al., 2006), fucoidan (Kim & Shin, 2015) and xylose (J. Liu & Jing, 2016).

1.6 Nano-bio interactions

Typically, research focuses on NP synthesis methods, drug release, encapsulation efficiency and observable effects like biodistribution or tumor shrinkage (Hao et al., 2014; Jithan et al., 2011; Kinsella et al., 2011; Noguchi et al., 1998; Sun et al., 2008). These are important topics in the design of NPs for pharmacological applications, but NPs are not exempt from interactions with biological systems during their lifetime (Prajitha et al., 2019).

Results like cancer-specific cytotoxicity could originate from the bioactive properties of the encapsulated/delivered compound, but it could also be a consequence of NP-cell interactions. A very similar concern was brought up by Leroueil et al. (2008), as they recognized the challenge of not disrupting cell membranes while having efficient NP permeability, and further discussed by Contini et al. (2018). Another study investigated NP adhesion to cell membranes and supported lipid bilayers and concluded that adhesion is a crucial step that leads to NP internalization (Lesniak et al., 2013). Even though some progress has been made to understand NP-cell interactions, there is still a gap in physicochemical interactions between NPs and other biological components whose role *in vivo* also determine NP uptake and bioaccessibility.

Mucosal surfaces are a physical barrier between exogeneous compounds like nanocarriers and biological systems, still many drugs and carriers are designed to be administered through the mucosa because this kind of delivery is less invasive and improves bioavailability (Khutoryanskiy,

2018). In the GIT, mucosal surfaces are lined with a mucus gel layer that lubricates and protects the stomach and intestine (Allen & Pearson, 2000). The narrow shape of the intestine and its length favors interactions of particles with the mucus layer (van der Schans & Rubin, 2004), but curcumin has low absorption and rapid metabolism in the intestine (Cas & Ghidoni, 2019). Therefore, protecting curcumin from degradation is not sufficient to increase its bioavailability *in vivo*. To promote curcumin uptake in the intestine, it is extremely important to understand the interactions happening between NP and the mucus layer.

Mucins are the major macromolecules in the mucus (Sigurdsson et al., 2013). They are glycoproteins with a remarkable structure that is composed of 50 – 80% carbohydrates and confers the molecule a high molecular weight between 0.5 and 50 MDa (Bromberg & Barr, 2000; Corfield, 2000). The oligosaccharide chains are linked to oxygen and nitrogen atoms of the polypeptide backbone (Sambrook et al., 1993). Mucin regulates the intake of molecules through selective interaction (Dekker et al., 2000), thus making it a great model to investigate bio-nano interactions.

Khanvilkar et al. (2001) reported that many factors influence which compounds will go through the mucus into the epithelial cells, including gel structure of the mucus and cross-linking between mucins. One factor that stands out in determining nano-bio interactions with mucin is the size and charge of particles. It has been reported that molecules with higher molecular weight and/or size show more difficulty crossing the mucus layer. Additionally, mucins are negatively charged and tend to bind to cationic particles through electrostatic interactions (Khanvilkar et al., 2001). Strong interactions with mucin can result in full elimination of NPs because the mucus layer is constantly renovated (Corfield, 2000). However, if NPs do not interact with mucin at all in solution, it is unlikely that it will show interactions *in vivo* (Hounsell, 1993; Pearson et al., 2000).

1.7 Hypothesis and objectives

It is hypothesized protein interactions with curcumin will be affected by glycation as a result of conformational changes. Because glycation is not expected to happen in the hydrophobic core of BSA, protein-curcumin interactions should not be directly impaired by glucose. The chemical modification of BSA shall modify physicochemical characteristics thus resulting in different NP interactions with mucin, compared to native BSA NPs. The objective of this thesis is to observe the effects of glycation on protein characteristics and understand how chemical modification affects interactions with hydrophobic compounds using curcumin as a model. Lastly, the thesis aims to evaluate whether glycation impacts or not the interactions between protein NPs and mucin.

Chapter 2

Materials and methods

2.1 Materials

8-Anilo-1-naphthalenesulfonic acid (ANS), ethanol, curcumin (Cur, ≥94% purity), o-phthaldialdehyde (OPA), lectin from *Triticum vulgaris*, Tween® 20, bovine serum albumin (BSA, 96% purity), D-(+)-glucose, L-serine, DL-dithiothreitol (DTT), glycerol (≥99.0%), glycine (≥99.0%), sodium phosphate monobasic (≥98.0%), sodium phosphate dibasic (≥98.5%), bromophenol blue, acrylamide/bis-acrylamide (30% solution), tris base (≥99.9%), methanol, acetic acid, ammonium persulfate (≥98%), N,N,N',N'-tetramethylethylenediamine ReagentPlus® (99%), mucin from porcine stomach (Type III), β-mercaptoethanol (≥99.0%), sodium dodecyl sulphate bioreagent (SDS) (≥98.5%), hydrochloric acid (37%) and di-sodium tetraborate decahydrate were obtained from MilliporeSigma Chemical Co. Ltd. (Oakville, ON, Canada). Coomassie Brilliant Blue R-250 staining solution, DC™ Protein Assay and Precision Plus Protein™ Dual Xtra Prestained were purchased from BioRad Inc. (Mississauga, ON, Canada). Sodium hydroxide (≥98%) was purchased from Fisher Scientific Inc. (Ottawa, ON, Canada). Milli-Q water (18.2 MΩ cm resistivity at 25℃, total organic carbon level ≤5 ppb) was purified using a commercial water-purification system (Advantage A10 Q-POD Milli-Q Water System). All reagents used were of analytical grade and did not require further purification.

2.2 Methods

2.2.1 Protein glycation method

A 0.15 mM BSA solution with 150 mM glucose was adjusted to pH 7.2 (± 0.2) with 0.1 M sodium hydroxide. The vessel containing the BSA-glucose mixture was closed and incubated in a

water bath at 60℃ with agitation (50 rpm) for 6 h. Then, the vessel was immediately put in an ice bath to stop the reaction. The conjugate was dialysed against deionized water overnight at 4℃ in a dialysis tube (14 kDa molecular weight cut-off, Fisher Scientific Inc., Ottawa, Canada). The protein content was determined with DC™ Protein Assay, following the instructions from the manufacturer (BioRad, CA, USA).

2.2.2 Dynamic light scattering (DLS) analysis

The average particle size (Z-average), polydispersity index and zeta potential of BSA-glucose conjugates and native BSA were investigated by dynamic light scattering using Nano-ZS Zetasizer (Malvern Instruments Ltd., Malvern, UK). Samples were diluted to 1 mg/mL in Milli-Q water (pH 7, refractive index 1.330, viscosity 0.8872 cP and dielectric constant 78.5) to avoid multiple scattering. For determination of nanoparticle zeta potential, the nanoparticles were diluted to 1 mg/mL in PBS (at pH 7.2 or 6.0 ± 0.2 with the adequate NaCl concentration of either 0.1 or 150 mM). All measurements were taken in triplicates at 25℃ with the Smoluchowski model at F(ka) 1.50 and backscattered angle of 173º.

2.2.3 Surface hydrophobicity determination

The surface hydrophobicity of native and glycated BSA was determined through ANS relative fluorescence intensity using a Spark multimode microplate reader (Tecan, Stockholm, Sweden) (Alizadeh-Pasdar & Li-Chan, 2000). Briefly, 8 mM ANS solution and 2 mg/mL solutions of each sample were prepared in phosphate buffer (0.1 M, pH 7.4). Samples underwent serial dilutions to 1.0, 0.5, 0.25 and 0.125 mg/mL with the phosphate buffer. Then, 200 µL of diluted individual samples and 2 µL ANS were combined in each well. After 15 minutes of incubation in

the dark, the fluorescence intensity of ANS was measured at emission and excitation wavelengths of 470 and 390 nm, respectively. Afterwards, the fluorescence intensity spectra from 430 to 600 nm with an excitation of 390 nm was obtained (Gazme et al., 2020). The surface hydrophobicity was taken to be the slope of the linear fit ($R^2 > 0.99$) of fluorescence intensity vs. sample concentration plot (Alizadeh-Pasdar & Li-Chan, 2000).

2.2.4 Free amino group content determination

The quantification of free amino groups in BSA before and after glycation was determined through a reaction with *o*-phthaldialdehyde (OPA) and the reaction product has a maximum absorbance at 340 nm. In this study, the OPA method reported by Nielsen et al. (2001) was used to determine the free amino group content. The OPA reagent was prepared as follows: OPA was dissolved in ethanol (40 mg/mL) and added to a solution of di-Na-tetraborate decahydrate (38.1 mg/mL) with SDS (1.0 mg/mL) in deionized water to yield a final concentration of 0.8 mg OPA per mL. Then, DTT was added to a final concentration of 0.88 mg/mL.

From each sample (20 mg/mL), 30 µL was incubated with 225 µL of OPA reagent for 2 minutes at 25℃ with shaking. The absorbance at 340 nm was recorded with a Spark multimode microplate reader (Tecan, Stockholm, Sweden) immediately after the incubation. Serine solution at the concentration of 0.1 mg/mL was used as the standard (0.9516 mEq/L) and deionized water was used as the blank.

Serine's milliequivalent NH_2 per gram of protein (serine-NH_2) was calculated with Eq. 1, where A is the recorded absorbance; x is the mass of sample in grams; P is the sample's protein content and 0.1 is the sample volume in liters (Nielsen et al., 2001). Native BSA was considered to have 100% available amino groups as it is the control.

$$Serine\text{-}NH_2 = \frac{(A_{sample} - A_{blank})}{(A_{standard} - A_{blank})} \times 0.9516\ mEq/L \times 0.1 \times \frac{100}{x} \times P \qquad \text{Eq. 1}$$

The degree of glycation (DG) was calculated using Eq. 2 below (Pan, Li, et al., 2020; Pan, Wu, et al., 2020):

$$DG\ (\%) = \left(1 - \frac{Serine\text{-}NH_{2\ after\ glycation}}{Serine\text{-}NH_{2_{native\ BSA}}}\right) \times 100 \qquad \text{Eq. 2}$$

2.2.5 Fluorescence quenching analysis of curcumin-protein interactions

The fluorescence quenching technique (Bourassa et al., 2013; Kanakis et al., 2013; Okagu et al., 2020, 2021) was used to investigate the interactions of curcumin with native and glycated BSA. Curcumin stock solution in ethanol (2.7 mM) was serially diluted to 1 mM and then to 0.5 mM using deionized water. Native and glycated BSA were dissolved in water at a concentration of 0.25 mg/mL. To prepare aliquots for fluorescence spectroscopy, curcumin (0.5 mM) and water were combined with the sample of interest. The final curcumin concentration was between 0 and 100 µM, and all aliquots had a constant sample concentration of 0.125 mg/mL. The fluorescence spectra were recorded at 300 to 500 nm emission wavelength and 280 nm excitation wavelength using Varian Cary Eclipse spectrofluorometer (Agilent, Santa Clara, CA, USA). Tryptophan fluorescence intensity at 334 nm was used to calculate the binding parameters as shown below. All measurements were executed in triplicates.

The number of binding sites occupied by curcumin molecules (n) and the binding constant of the curcumin-protein complex (K_A) were estimated using Eq. 3. F and F_0 correspond to the fluorescence intensity with and without curcumin, respectively, and $[Q]$ is curcumin molar concentration (i.e., quencher molar concentration).

$$log\left[\frac{F_0 - F}{F}\right] = \log K_A + n\log[Q] \quad \text{Eq. 3}$$

The Stern-Volmer equation was used to determine the accessible fluorophore fraction (f) and the Stern-Volmer quenching constant (K) (Eq. 4).

$$\frac{F_0}{F_0 - F} = \frac{1}{fK[Q]} + \frac{1}{f} \quad \text{Eq. 4}$$

Lastly, the modified Stern-Volmer equation (Eq. 5) was used to determine the nature of the quenching in curcumin-protein complexes, as it can be either static or dynamic (Albani, 2007). With Eq. 5, the biomolecular quenching rate constant (K_Q) and the Stern-Volmer dynamic quenching constant (K_D) were estimated. In this equation, t_0 is the mean fluorescence lifetime of the fluorophore in the absence of curcumin (t_0 = 10^{-9} s) (Albani, 2007).

$$\frac{F_0}{F} = 1 + K_Q t_0[Q] = 1 + K_D[Q] \quad \text{Eq. 5}$$

2.2.6 Sodium dodecyl sulfate-polyacrylamide gel electrophoresis (SDS-PAGE)

The molecular weight profiles of glucose-BSA conjugates were investigated through SDS-PAGE with a 12% separating gel and 3% (w/v) stacking by adapting the method of Laemmli (1970). The sample buffer was prepared with glycerol, 10% (w/v) SDS, 0.5% (w/v) bromophenol blue, and 0.5 M Tris-HCl (pH 6.8). β-Mercaptoethanol was added to the sample buffer at a 1:19 v/v ratio. Glycated and native BSA solutions (4 mg/mL) were prepared with Milli Q water, followed by a 1:2 dilution with sample buffer. Then, the samples were heated at 95°C for 5 minutes. Thereafter, 10 µL of treated samples or Precision Plus™ Dual Xtra protein standard were loaded into each well. Protein separation was conducted at 150 V in a BioRad Mini-PROTEAN® Tetra Cell electrophoresis unit (BioRad Inc., Mississauga, ON, Canada). After washing three times with Milli

Q water, the gels were stained with Coomassie Brilliant Blue R250 (BioRad Inc., Mississauga, ON, Canada) overnight at room temperature with shaking (300 rpm). The gels were de-stained with a solution of water (50%), methanol (40%) and acetic acid (10%), and images were obtained using ChemiDoc™ (BioRad Inc., Mississauga, ON, Canada). The protein bands were analysed with ImageJ version 1.53e for Windows (NIH, USA).

2.2.7 Nanoparticle synthesis

Following a previously reported method (Okagu et al., 2020) with some modifications, protein samples were dissolved in Milli-Q water to a concentration of 5 mg/mL. A curcumin solution (1 mg/mL) was prepared in ethanol. Both the curcumin solution and curcumin-loaded nanoparticles were protected from light by wrapping the vessel with aluminum foil. For the synthesis of hollow nanoparticles, ethanol was added dropwise to the protein solution (1:10 volume ratio) with constant stirring at 320 rpm for two hours at room temperature. Curcumin-loaded nanoparticles were synthesized the same way, expect that the curcumin solution was added instead of pure ethanol. Nanoparticles were freshly synthesized and kept in solution for characterization and mucin-binding property assay.

2.2.8 Mucin-binding property assay

Immediately after synthesis, 200 µL of prepared nanoparticles was used to coat a Nunc MaxiSorp™ flat-bottom 96-well microplate overnight at room temperature. Wells were washed four times with 5 mM phosphate buffered saline containing 0.05% Tween 20 (PBST at pH 7.2), followed by blocking with 150 µL of 2% BSA solution in 5 mM phosphate buffered saline containing 150 mM NaCl (pH 7.2) for one hour at 37°C. The 2% BSA solution was used as the

negative control. Thereafter, the plate was washed four times with PBST and 200 µL of mucin suspension (10 mg/mL) was added to each well. The plate was then incubated for 24 hours at 37°C.

To understand the effects of different pH and ionic strengths on the interactions between nanoparticles and mucin, different mucin solutions were prepared. The pH of the intestine increases progressively from pH 6 to 7.4, thus pH 6.0 and 7.2 were chosen to mimic two different physiological conditions (Fallingborg, 1999). Furthermore, the ionic strength of biological fluids is not constant therefore two distinct concentrations were considered: 0.1 and 150mM NaCl.

Briefly, a stock 5 mM PBS solution was used to yield 5 mM PBS at pH 7.2 and 6.0 (± 0.2). Then, each PBS solution was used to make a low ionic strength (0.1 mM NaCl) and a high ionic strength (150 mM NaCl) solutions, totalling four different conditions. Mucin was hydrated in PBS buffer with stirring at 600 rpm for one hour.

For all assays, the plate was washed four times with PBST and 100 µL of 25 µg/mL FITC labeled wheat germ agglutinin (FITC-WGA) prepared in PBS was added to each well. The plate was covered with aluminum foil and, after 30 minutes, washed three times with PBST and once with PBS. Next, 100 µL of PBS was added to the wells and fluorescence intensity was measured immediately from the bottom of the plate to estimate the amount of FITC-WGA bound to mucin at excitation wavelength of 494 nm and emission wavelength of 518 nm (Spark multimode microplate reader, Tecan, Stockholm, Sweden). The mucin-binding property of sample was calculated using the following ratio:

$$Binding\ property = F/F_0 \qquad \text{Eq. 6}$$

F is the fluorescence intensity of FITC-WGA in the presence of the sample and F_0 is the fluorescence intensity of the negative control (without adding the samples).

2.2.9 Statistical analysis

Protein glycation was conducted in triplicate and subsequent analysis were also conducted in experimental triplicates. Data were expressed as mean ± standard deviation. T-test and ANOVA statistical analyses were performed using GraphPad Prism version 9.1.1 for Windows (GraphPad Software, La Jolla, CA). Significant differences were established considering $P \geq 0.05$ as not significant.

Chapter 3

Results and discussion

3.1 Characterization of glycated bovine serum albumin

3.1.1 Free amino group contents of native BSA and BSA-glucose conjugates

To quantify the amino groups in the produced conjugates, determining the protein content of the samples is essential. Amino groups involved in the Maillard reaction become unavailable as observed in Figure 1.3. Since only the free amino groups can be quantified through the OPA assay (Ledesma-Osuna et al., 2008; Nielsen et al., 2001), a reduction in OPA absorbance is directly related to glucose molecules binding to the protein.

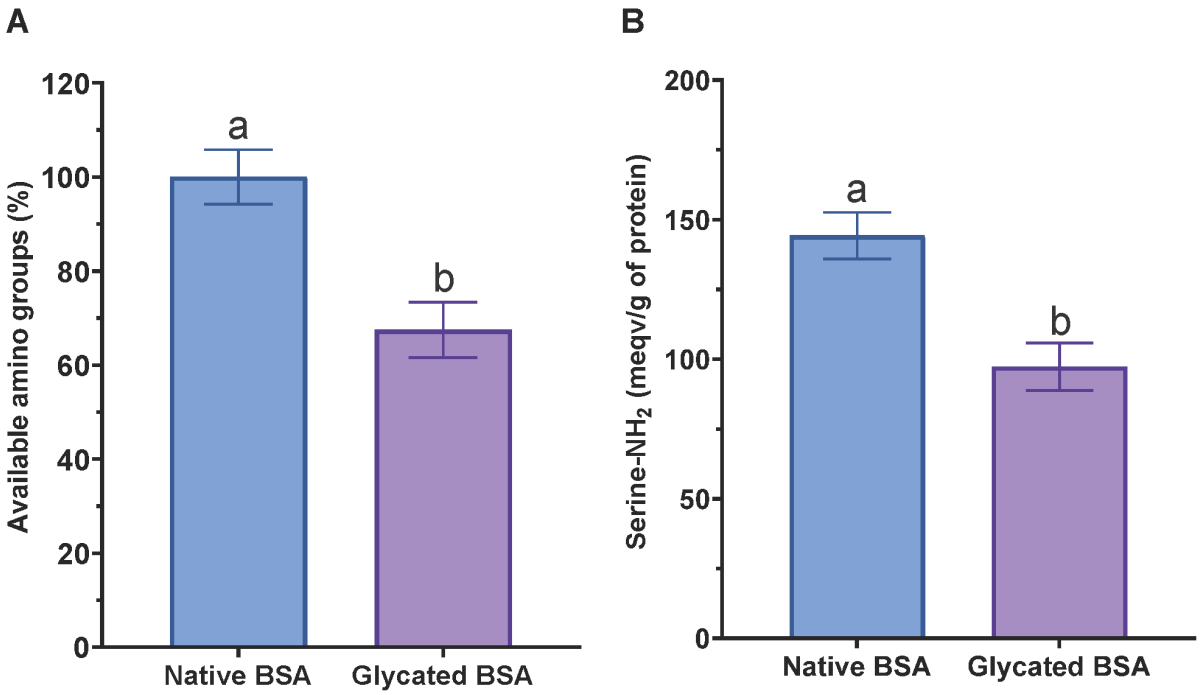

Figure 3.1 Normalized available amino groups and estimated serine-NH_2 equivalent of native and glycated BSA in graphs A and B, respectively.

Bars represent average value ± standard deviation (n=3, experimental replicates) and, for each graph, mean values with a letter in common are not significantly different according to T-test ($P \geq 0.05$).

Figure 3.1A depicts the percentage of free amino groups in native BSA and its conjugate with glucose. After 6 hours of glycation, around 67% of the free amino groups in BSA remained available and the actual serine-NH_2 mEq per gram of protein calculated with Eq. 1 experienced a very significant decrease (depicted in Figure 3.1B). Therefore, the OPA assay confirms that glucose bound to the amino groups of BSA.

Ledesma-Osuma et al. (2008) reported that around 70% of BSA amino groups remained free after approximately 4 hours of dry-heating glycation with glucose. Longer reaction time decreases the amount of free amino groups. Although wet-heating method was used in this work, our results are in line with the reported value.

Reaction conditions, such as temperature or time, are a few of many factors reported to influence the extent of glycation (DG), i.e. carbohydrate reactivity (Ledesma-Osuna et al., 2008; Zhang et al., 2019). Researchers have shown that DG of BSA with monosaccharides decreases in the following order: BSA-xylose > BSA-galactose > BSA-glucose (J. Liu & Jing, 2016). Galactose is also slightly more reactive than glucose in the glycation of β-lactoglobulin (Chevalier, Chobert, Genot, et al., 2001; Chevalier, Chobert, Popineau, et al., 2001).

The estimated DG of BSA-glucose conjugates is of 33 ± 6%. A lower DG was obtained for β-lactoglobulin-dextran conjugates and whey protein isolate-gum acacia conjugates at 6.7 and 28.14%, respectively (Chen, Ma, et al., 2019; Yi et al., 2014). DG is directly related to the size of sugar molecules. A lower DG is result of the difficulty of larger sugars to diffuse and bind to amino groups due to steric hindrance (Wong et al., 2011). In particular, glucose yields a considerably high DG because its short carbonic chain exists more commonly in open chain forms than bigger carbohydrates (Chevalier, Chobert, Popineau, et al., 2001).

3.1.2 Surface hydrophobicity of native BSA and BSA-glucose conjugates

Conformational changes in the protein are indicated through the measurement of surface hydrophobicity (Chen, Lv, et al., 2019; Gazme et al., 2020). The more surface hydrophobic groups a protein has, the higher the ANS fluorescence intensity (Albani, 2007; Matulis & Lovrien, 1998; Moro et al., 2001). Because glycation was accelerated at 60°C, a higher surface hydrophobicity could be expected as the protein unfolds and exposes its core hydrophobic groups (Kim & Shin, 2015). However, surface hydrophobicity decreased after glycation as revealed by the decrease in ANS relative fluorescence intensity (see Figure 3.2 and Figure 3.3).

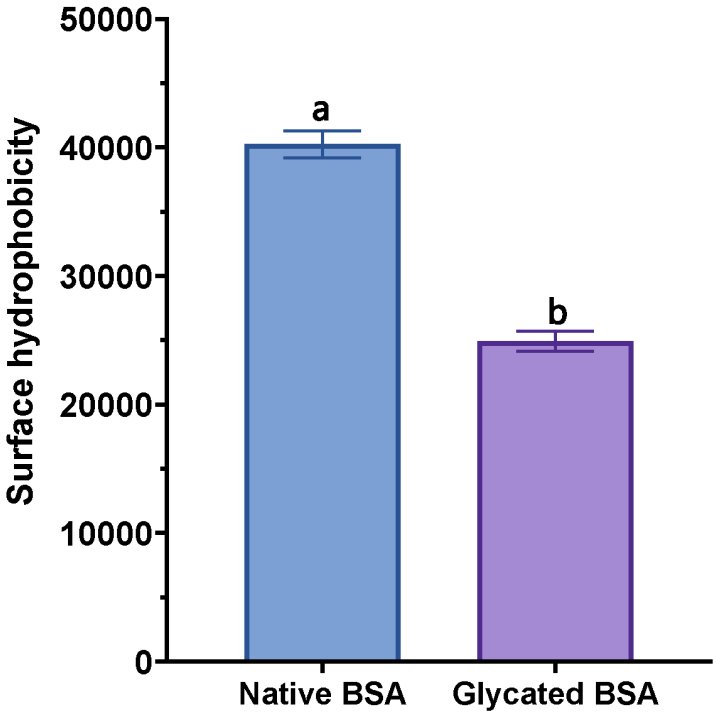

Figure 3.2 Estimated surface hydrophobicity.

Bars represent average value ± standard deviation (n=3, experimental replicates) and values with a letter in common are not significantly different according to T-test ($P \geq 0.05$).

This result is in accordance with the literatures that reported reduced surface hydrophobicity of other carbohydrate-protein conjugates such as WPI-gum acacia and WPI-maltodextrin conjugates (Chen, Lv, et al., 2019; G. Liu & Zhong, 2012; Yang et al., 2018). The possible explanation is that the electrostatic binding of ANS anions to positively charged residues is obstructed by glucose. A steric shielding has been suggested before to interfere with hydrophobicity activity on the protein surface (Wong et al., 2011). Additionally, the conjugation of glucose to positively charged Lys results in loss of net cationic charges thus reducing electrostatic interactions with ANS. The hydrophilic OH groups of glucose also contribute to the increased hydrophilic profile of the protein conjugates (Chen, Lv, et al., 2019; G. Liu & Zhong, 2012).

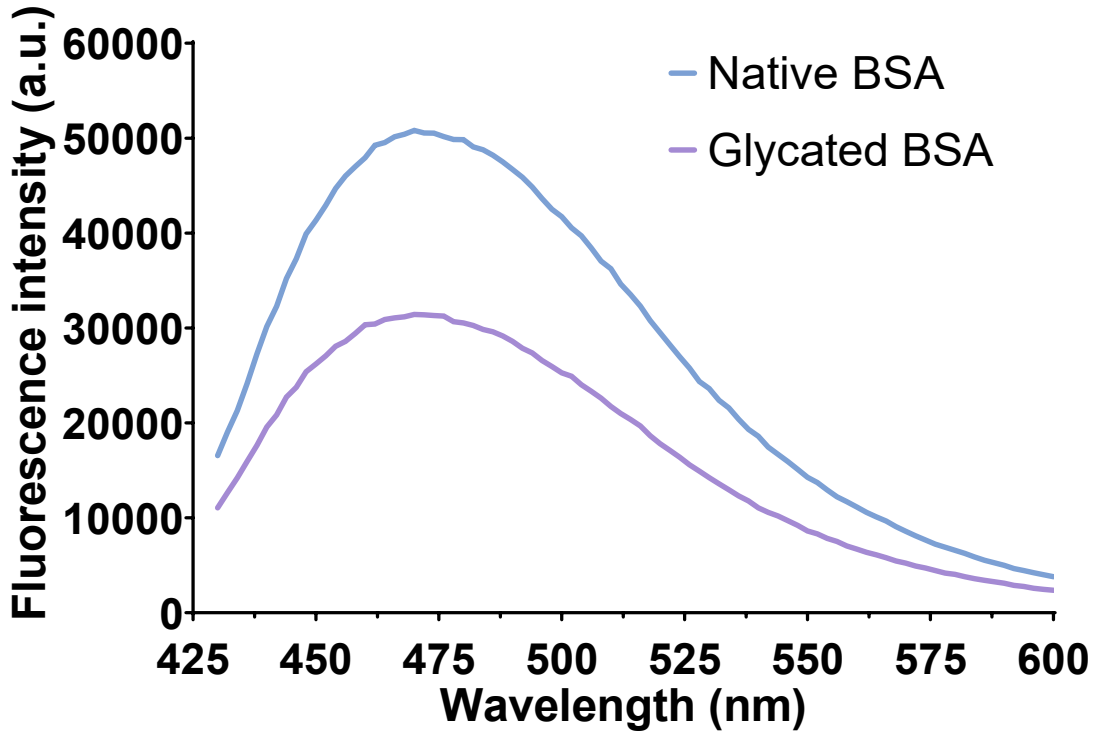

Figure 3.3 ANS fluorescence intensity spectra of native and glycated BSA.

The graph depicts one out of three readings.

3.1.3 Surface charge, mean particle diameter (Z-average) and polydispersity index (PDI) of native BSA and BSA-glucose conjugates

Zeta potential and net surface charge were evaluated to indicate the physicochemical changes due to glycation (Fan et al., 2018). As shown in Figure 3.4A, glycation resulted in a significant increase in surface charge magnitude. Lysine is a positively charged residue and the subsequent interaction with glucose results in charge neutralization (Figure 1.3). Liu & Zhong (2013) reported a significant decrease in the amount of lysine residues in WPI after conjugation with glucose accompanied by a reduction in zeta potential (G. Liu & Zhong, 2013). Comparable surface charges were reported after glycation of BSA with other monosaccharides, -15.0 and -15.2 mV for BSA-xylose and BSA-galactose conjugates respectively (J. Liu & Jing, 2016).

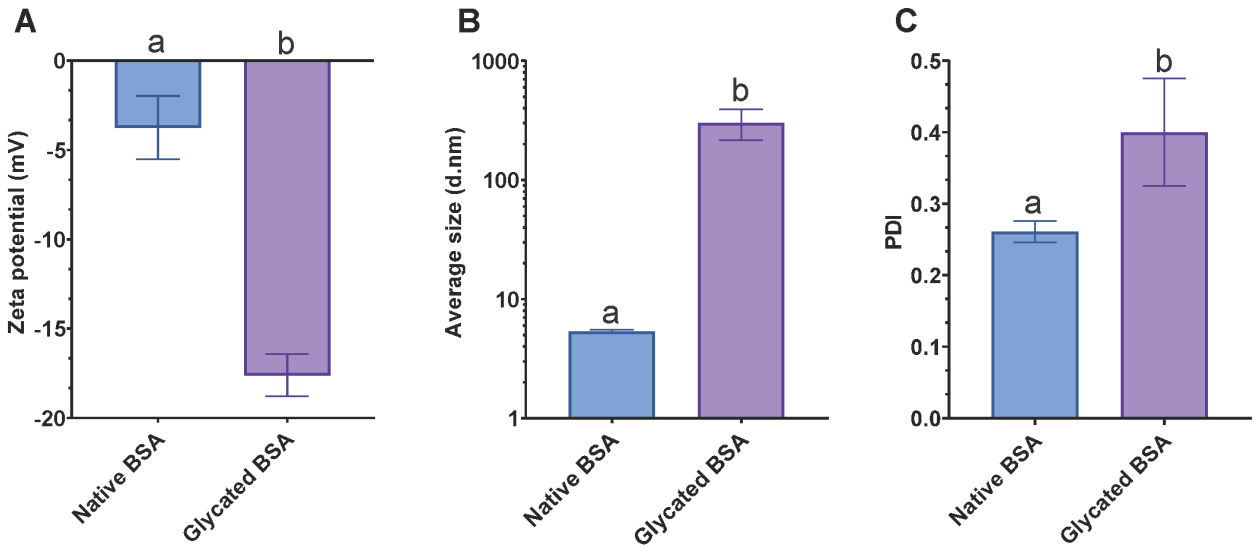

Figure 3.4 Surface charge, mean particle diameter (Z-average) and polydispersity index (PDI) of native BSA and BSA-glucose conjugates in plots A, B and C, respectively.

Values are shown as average ± standard deviation (n=3, experimental replicates). For each graph, mean values with a letter in common are not significantly different according to T-test ($P \geq 0.05$).

Native BSA showed a more monodisperse particle distribution and a smaller particle size compared to the conjugates, with PDIs of 0.261 and 0.400, and Z-average of 5.38 ± 0.15 and 302.58 ± 87.89 d.nm, respectively (Figure 3.4 B and C). It is possible that cross-linking between protein molecules took place during glycation, which induced the rise of PDI and particle size. As illustrated in Figure 3.5, the size distribution of BSA-glucose conjugates shifted towards bigger diameter sizes compared to native BSA, which is consistent with the results of average particle size (Figure 3.4B).

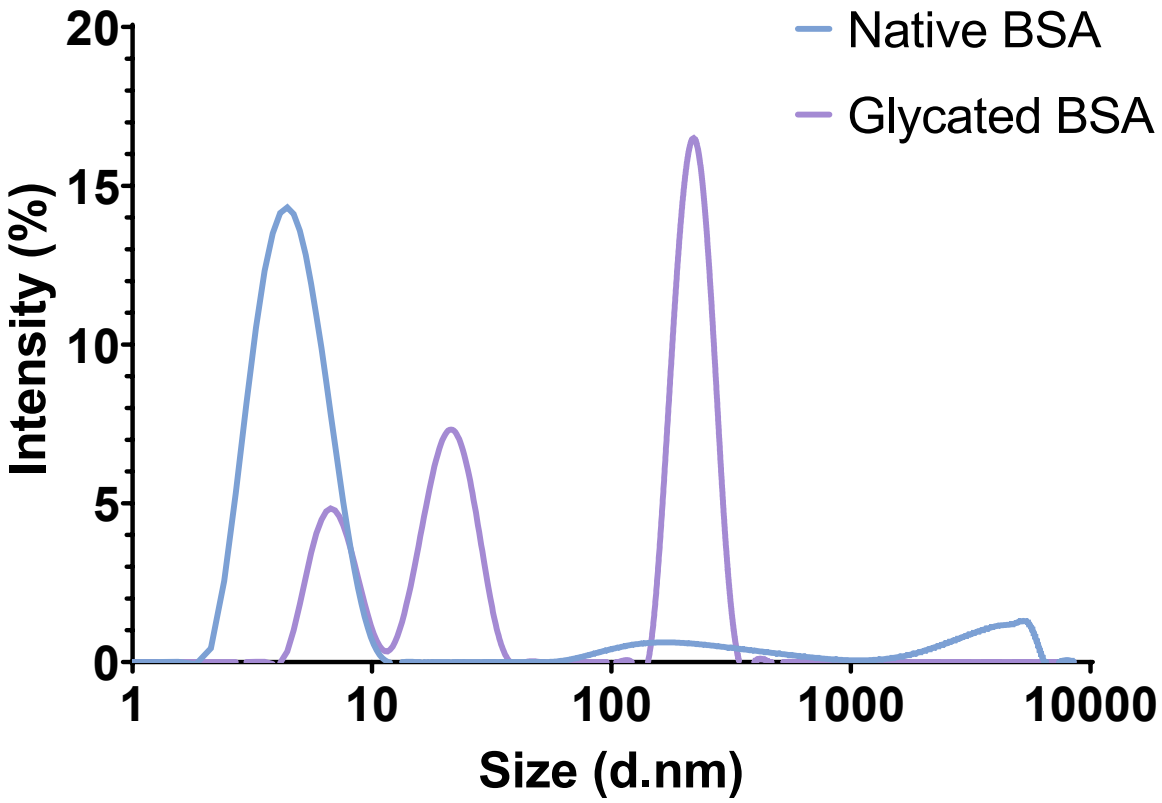

Figure 3.5 Size distribution of native BSA and BSA-glucose conjugates.

The graph depicts one out of three readings.

In Figure 3.5, two peaks at around 200 and 1,400 d.nm were detected from the native BSA sample that could be a result of a modest molecular aggregation, which is consistent with the low net surface charge of -3.75 mV. Reduction in electrostatic repulsion often causes particle interaction and aggregation (Fan et al., 2018; Salehiabar et al., 2018). Thus, compared to pure BSA, the lack of peaks above 400 d.nm from the conjugate sample could be explained by the stronger electrostatic repulsion due to its higher zeta potential. Moreover, a few authors discussed the possibility that glycation may hinder the extent of particle aggregation because of the sugar steric hindrance and this effect has been reported for BSA-glucose conjugates as well (Fan et al., 2018; G. Liu & Zhong, 2012; Rondeau et al., 2007).

3.1.4 Effect of glycation on the BSA profile

As seen in Figure 3.6, the main band of BSA, at 66 kDa, appears more compact for the glycated sample, which has also been reported by Kim et al. (2015). The patterns seen are coherent with the surface modification because the small molecular weight of glucose, compared to albumin, is not expected to be observable in the gel. Besides, the lack of new bands above 75 kDa indicated absence, or minimal presence, of intensive cross-linking between conjugates by disulfide bonds. Thus the molecular weight distribution of the BSA-glucose conjugate in Figure 3.6 is consistent with the observations from Figure 3.5 that BSA-glucose samples lack peaks above 400 d.nm in the particle size distribution graph, meaning that agglomeration and intensive cross-linking did not occur.

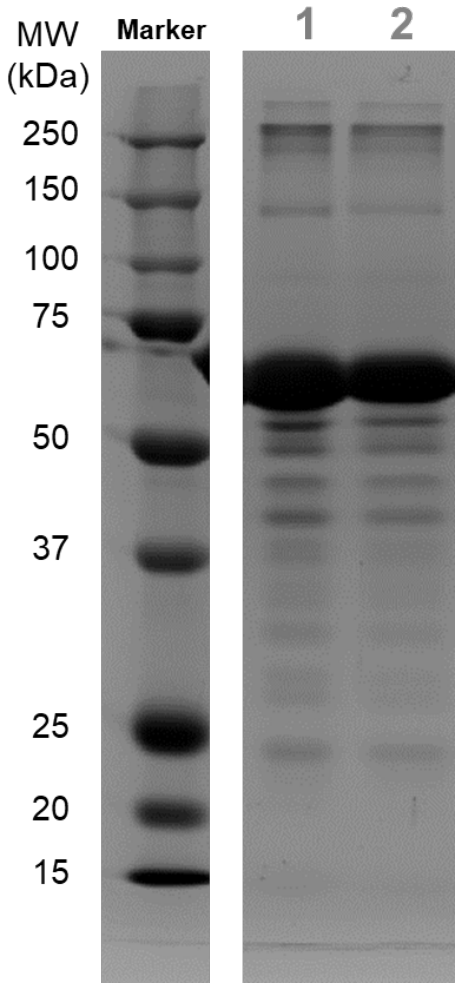

Figure 3.6 SDS-PAGE gel image after electrophoresis of native and glycated BSA.

Native BSA and glycated BSA are in lanes 1 and 2, respectively. The first column ("Marker") depicts the bands and their respective molecular weight (MW) in kDa are on the left.

3.2 Glycation effect on protein-curcumin interactions

Monitoring the changes in the intrinsic fluorescence of proteins is a pertinent tool in the studies of intermolecular binding and interaction, as well as the effect of such molecules on protein conformation. Intrinsic fluorescence is often measured through tryptophan, a fluorophore residue with a characteristic excitation peak at 280 nm and whose photophysical response is sensitive to the surrounding environment (Kanakis et al., 2013; Liang et al., 2008; Vivian & Callis, 2001).

3.2.1 Intrinsic fluorescence of BSA-glucose conjugates

In BSA, tryptophan (Trp) is found close to the surface (Trp-134) and within the hydrophobic core (Trp-212) (Albani, 2007; Kim & Shin, 2015; Tayeh et al., 2009). Because of the sensitivity of tryptophan, changes in protein conformation triggered by glycation are revealed in the intrinsic fluorescence emission spectra (Figure 3.7).

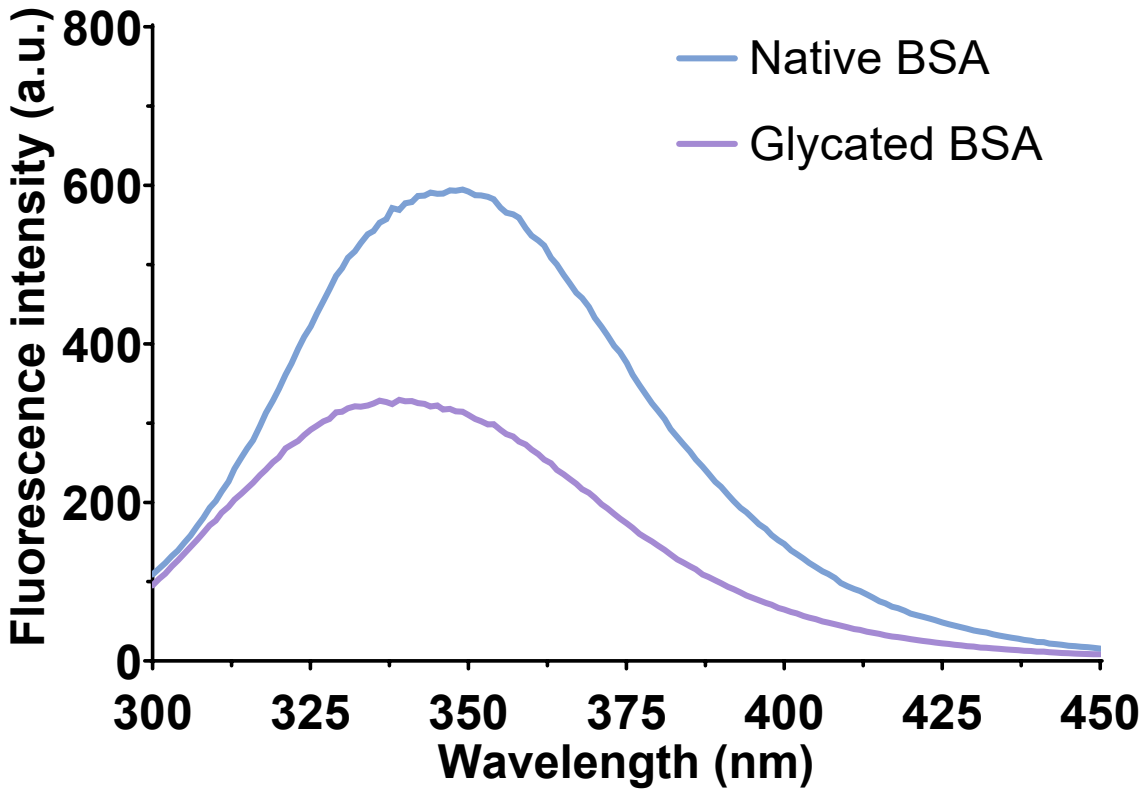

Figure 3.7 Tryptophan fluorescence emission intensity of native and glycated BSA in water. Spectrum shown is one out of three readings.

The movement of Trp from a polar to a nonpolar environment is generally expressed as a blue shift in wavelength maximum (λ_{max}) accompanied by an increase in fluorescence intensity (Liang et al., 2008; Vivian & Callis, 2001). However, in Figure 3.7, a minor λ_{max} blue shift from

349 to 339 nm is paired with a decrease in intensity in the glycated-BSA conjugate, compared to native BSA. This indicated a concurrent internalization of the fluorophore with interference in its fluorescence.

Bound glucose causes a shielding effect on the fluorescence of tryptophan (Chen, Lv, et al., 2019; Jung et al., 2006; Kim & Shin, 2015), which justifies the 44.6% decrease in fluorescence intensity (Figure 3.7). For BSA, Trp fluorescence quenching intensifies with higher glucose content, as shown by Rondeau et al. (2010). Compared to galactose, glucose is more effective in shielding the intrinsic fluorescence of BSA, i.e. galactose does not reduce the fluorescence of Trp as much as glucose.

BSA-dextran conjugates in the literature presented reduction in Trp fluorescence intensity to a greater extent (Jung et al., 2006). If the difference lies on the smaller size of monosaccharides such as glucose as opposed to polysaccharides like dextran, then it is arguable that monosaccharides incite a more modest shielding and structural alteration to BSA than its larger counterpart. In combination, the shielding effect and Trp internalization explain the decrease in surface hydrophobicity in addition to the observed fluorescence quenching (Ervin et al., 2000; Vivian & Callis, 2001).

3.2.2 Binding of curcumin to BSA-glucose conjugates

Similarly, the introduction of biomolecules that interact with the protein can be investigated through intrinsic fluorescence emission. Biomolecules capable of reducing intrinsic fluorescence intensity are known as quenchers and curcumin is known to have this effect in proteins (Liang et al., 2008; Okagu et al., 2021).

While a blue shift is seen after glycation in the absence of curcumin Figure 3.7, no shift is observed when curcumin is added to pure and glycated BSA solutions (Figure 3.8 A and B respectively) regardless of quencher concentration. In contrast, the fluorescence intensity is dependent on curcumin concentration in a way that higher curcumin concentrations lead to a decrease in fluorescence emission intensity.

Curcumin quenching effect is greater in native BSA (Figure 3.8A) even at the lowest curcumin concentration at 5 μM. The extent of quenching for the glycated counterpart (Figure 3.8B) may be a consequence of steric hindrance caused by glucose or a result of curcumin-glucose interactions. Nonetheless, glycation did not impair interactions between BSA and curcumin.

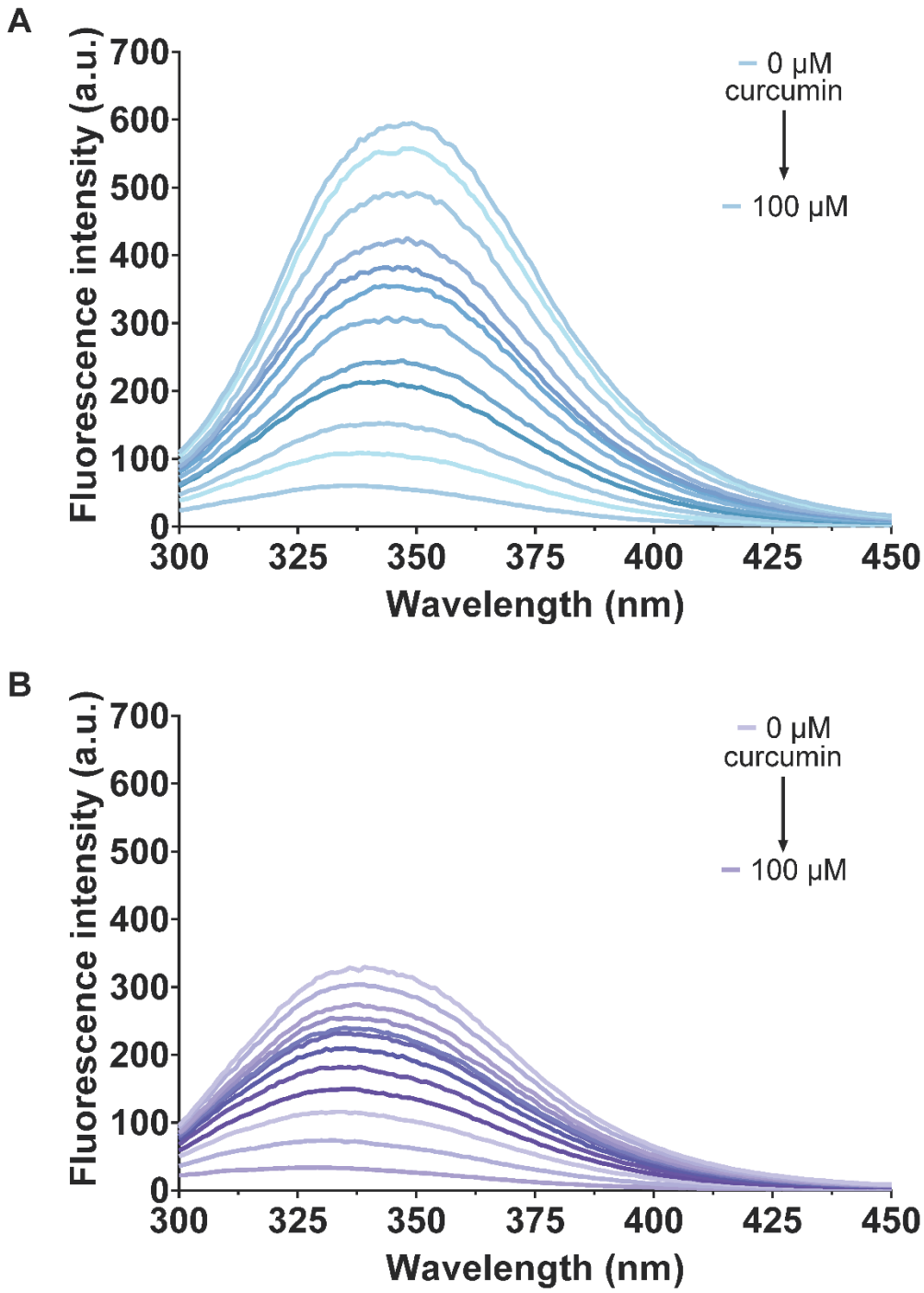

Figure 3.8 Fluorescence emission spectra of A) native BSA and B) glycated BSA in the presence of various curcumin concentrations.

The fluorescence spectra were recorded at 25℃ in triplicates. The main graphs depict one out of three readings. Curcumin concentration ranges from 0 to 100µM, increasing in 5µM increments until 30µM, in 10µM increments until 60µM and then in 20µM increments until 100µM. The

Stern-Volmer quenching constant (K) was calculated from $F_0/(F_0-F)$ against 1/[Curcumin] plot inserts (Eq. 4), and values are shown as average ± standard deviation (n=3, experimental replicates).

The Stern-Volmer quenching constant (K) can be interpreted as the binding affinity between curcumin and the samples (Okagu et al., 2021), and the respective values are arranged in Table 3.1. The increase in K from 0.99×10^4 M^{-1} to 3.63×10^4 M^{-1} after glycation points to a stronger bond within that complex. Collectively, K values, the concentration-dependent decrease in Trp fluorescence intensity, and lack of peak shifting imply that curcumin is binding to the protein in a manner that hinders the fluorescence of Trp residues without directly binding to Trp. In other words, since Trp is less available for interactions with curcumin after glycation but bonds with the protein are more recurrent and stronger, there must be another type of interaction between quencher and protein (Sneharani et al., 2010).

Table 3.1 Calculated fluorescence quenching parameters.

	K ($\times10^4$ M^{-1})	K_D ($\times10^4$)	K_Q ($\times10^{13}$ $M^{-1}s^{-1}$)	n	f
Native BSA	0.99 ± 0.23^a	3.15 ± 0.13^a	3.15 ± 0.13^a	1.54 ± 0.02^a	2.05 ± 0.37^a
Glycated BSA	3.63 ± 0.89^b	2.09 ± 0.02^b	2.09 ± 0.02^b	1.21 ± 0.03^b	0.70 ± 0.09^b

Where K is the Stern-Volmer quenching constant, K_D is the Stern-Volmer dynamic quenching constant, K_Q is the biomolecular quenching rate constant. n and f correspond to the number of binding sites taken by the quencher and the accessible fluorophore fraction, respectively. Values are shown as average ± standard deviation (n=3, experimental replicates) and values with a letter in common within the same column are not significantly different according to the T-test performed ($P \geq 0.05$).

A direct relationship between curcumin binding affinity and protein surface hydrophobicity has been considered where reduced hydrophobicity is linked to less curcumin-BSA complexes being formed (Okagu et al., 2021). However, a different trend is observed in Table 3.1. Although surface hydrophobicity reduced upon glycation (Figure 3.2), K increases significantly. It is

arguable that conformational changes, cross-linking, and steric hindrance caused by glucose act in combination and restrict the access to hydrophobic pockets in the protein. Consequently, the interactions seen between curcumin and the conjugate may not be of hydrophobic nature.

Simplistically, static quenching expresses the binding of curcumin, whist collisions are indicated by a pronounced dynamic quenching (Albani, 2007). The biomolecular quenching rate constants (K_Q) of pure and glycated BSA are both greater than the reported maximum static quenching of various macromolecule-quencher combinations (2×10^{10} $M^{-1}s^{-1}$) (Albani, 2007; Mohammadi et al., 2010; Okagu et al., 2020, 2021). In this study, binding forces are predominantly driving the fluorescence quenching, even though the number of curcumin molecules bound to albumin decreased significantly (Table 3.1 and Figure 3.9).

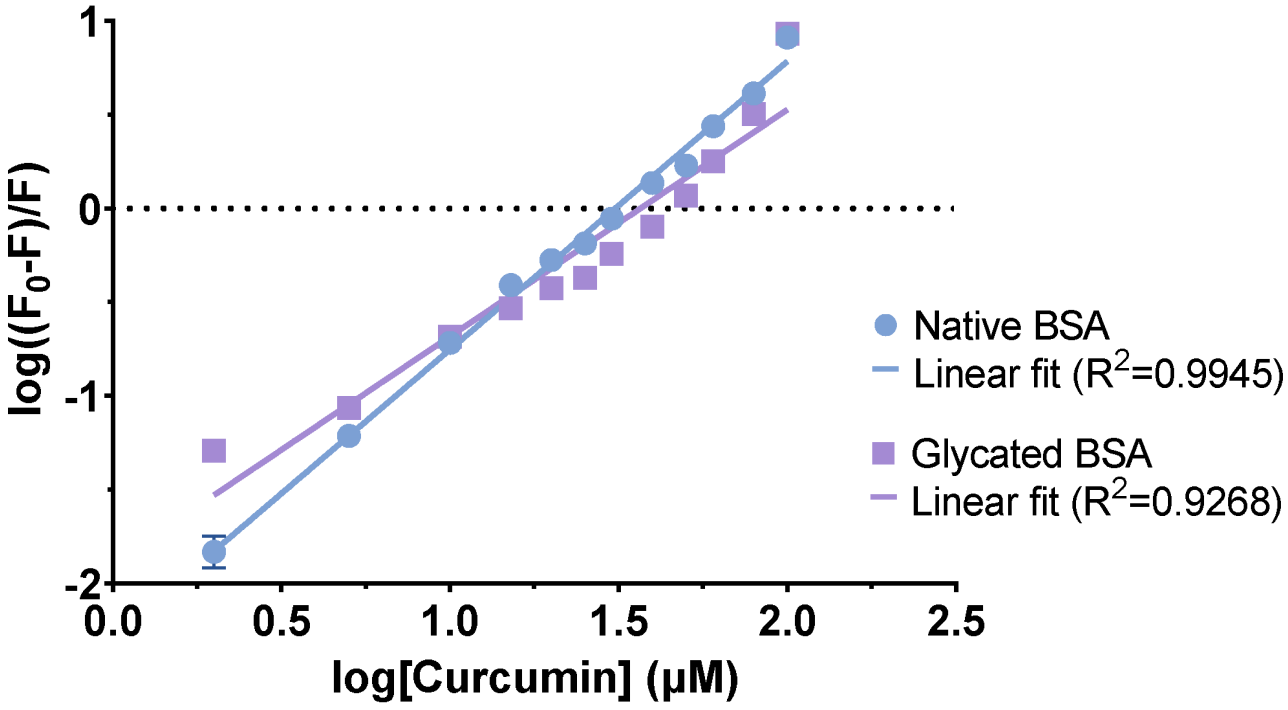

Figure 3.9 Plot of log((F₀-F)/F) as a function of log[curcumin] in µM.

Linear fit of native and glycated BSA were used along with Eq. 3 to estimate the number of curcumin molecules bound (n) to the protein. Values are depicted as average ± standard deviation (n=3, experimental replicates).

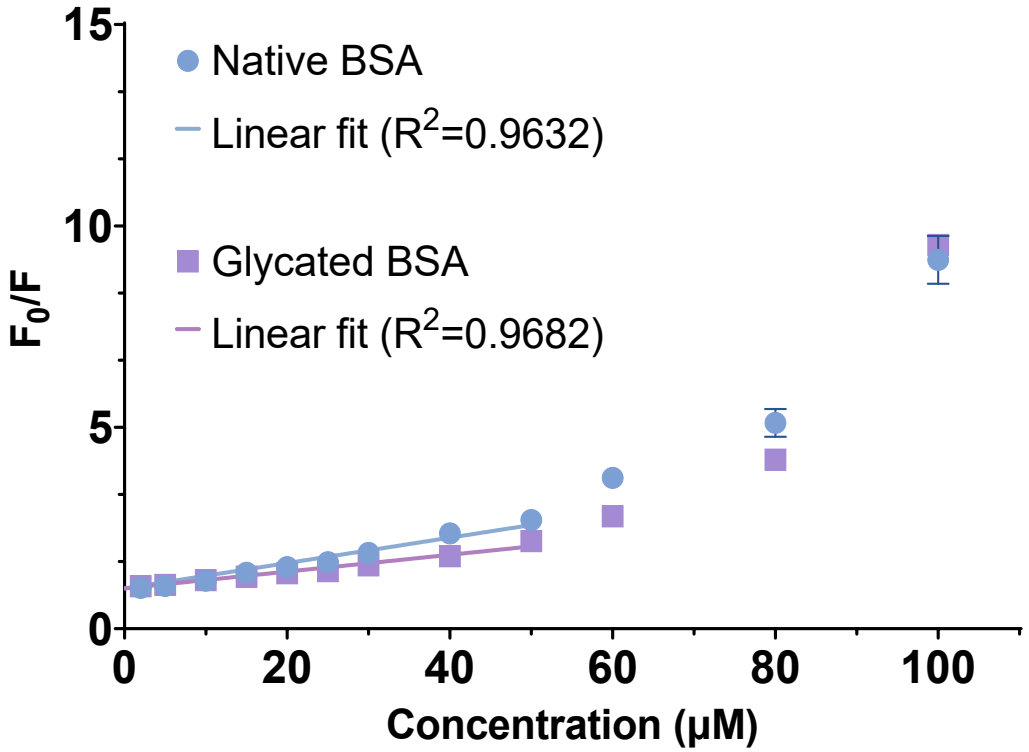

Figure 3.10 Stern-Volmer plot for native and glycated BSA.

Biomolecular quenching rate constants (K_Q) and Stern-Volmer dynamic quenching constants (K_D) were determined using the linear fits and Eq. 5. Values are depicted as average ± standard deviation (n=3, experimental replicates).

In Figure 3.10, the linearity of the plots when curcumin concentration is between 0 and 50 μM signifies a static nature of quenching (Albani, 2007; Okagu et al., 2020, 2021), whereas dynamic quenching is observed at concentrations above 50 μM. Comparable behaviour has been reported in β-lactoglobulin fluorescence quenching experiments with curcumin, where static quenching was also observed at curcumin concentrations below 50μM (Kanakis et al., 2013). Moreover, the quenching constant calculated by Kanakis et al. for BLG-curcumin is comparable to the one shown in Table 3.1, 3.3×10^{13} $M^{-1}s^{-1}$ and $3.15 \pm 0.13\times10^{13}$ $M^{-1}s^{-1}$ respectively.

The Stern-Volmer dynamic quenching constant (K_D) was estimated using the linear fits from Figure 3.10 and Eq. 5. Results are organized in Table 3.1. Given that K_D expressed a reduction in the presence of glucose, it is reasonable to postulate that more nonfluorescent complexes are formed with glycated BSA than with native BSA (Okagu et al., 2020). This result also supports the stronger binding affinity described previously in Table 3.1 and inserts in Figure 3.8.

The most hydrophobic residues are typically found in the core of the protein as a natural consequence of protein folding. As means to avoid exposure to the aqueous environment, curcumin preferentially interacts with albumin at the hydrophobic core (Sułkowska, 2002). The accessible fluorophore fraction (f, Table 3.1) quantifies tryptophan residues available for interactions with curcumin. The very significant decrease in f represents an internalization of core Trp residues (Albani, 2007), resulting in the inability to interact with curcumin. Despite this, more and stronger interactions were made between glycated albumin and curcumin likely in the formation of hydrogen bonds.

3.3 Mucin-binding property of nanoparticles at different physiological conditions

The mucus layer is located on the surface of epithelial tissues and acts as the lubricant and protective layer (Allen & Pearson, 2000). Recent study suggested that mucus layer plays an important role in regulating the intake of molecules through selective interaction (Dekker et al., 2000). Mucins are glycoproteins secreted by mucus-producing cells and correspond to the major macromolecules of mucus layer (Hounsell, 1993; Huet et al., 2000). Thus, mucin-binding property of nanoparticles at different physiological conditions were evaluated in this work.

Two intestinal pHs were selected: pH 6.0 corresponds to the small intestine, while pH 7.2 represents the terminal ileum (Fallingborg, 1999b). The effect of different ionic strengths on the interactions was also taken into consideration with 0.1 and 150 mM NaCl. Figure 3.11 illustrates the mucin-binding assay with nanoparticles.

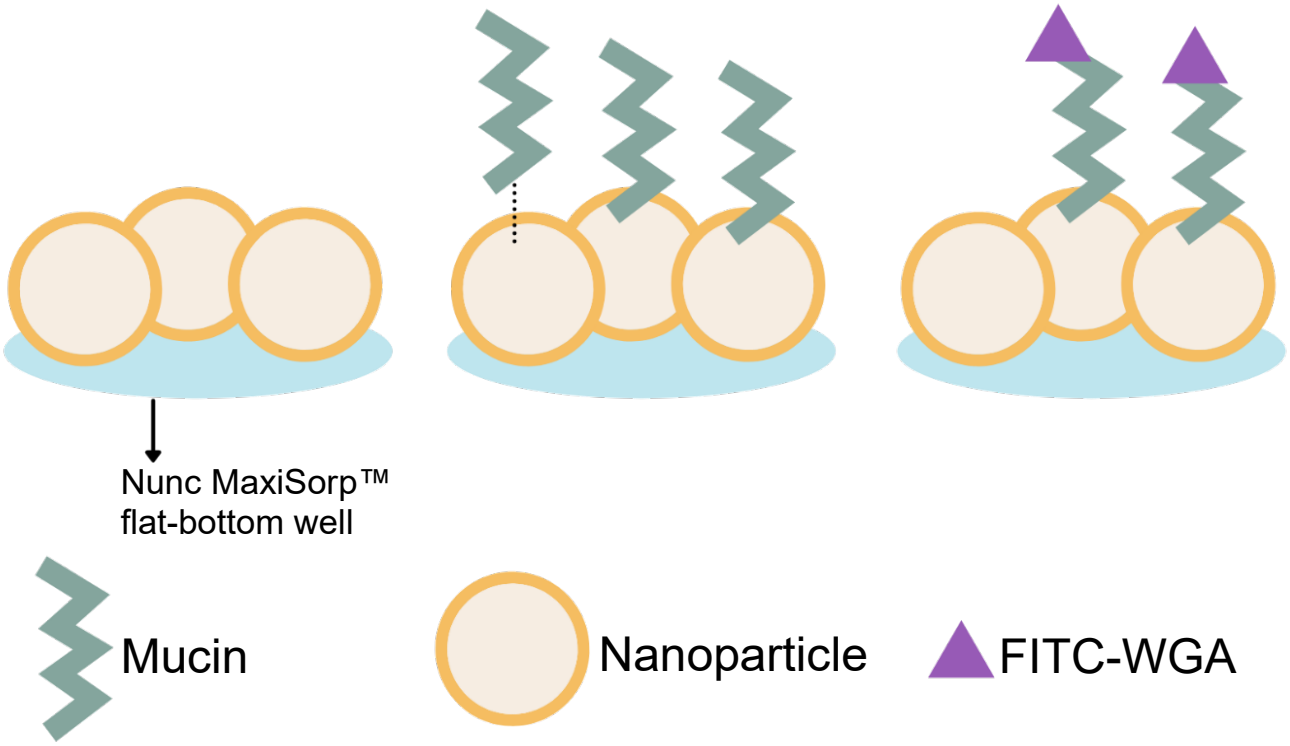

Figure 3.11 Schematic representation of the mucin-binding assay.

Scheme on the left represents nanoparticles bound to the well, to which mucin was added (center). Weak electrostatic interactions between mucin and nanoparticles are represented by the dotted line (center), whereas mucin bound to the NP is represented by mucin directly attached to the particle (center and right schemes). The scheme on the right represents only the bound mucin that remain after washing and FITC-WGA bound to mucin.

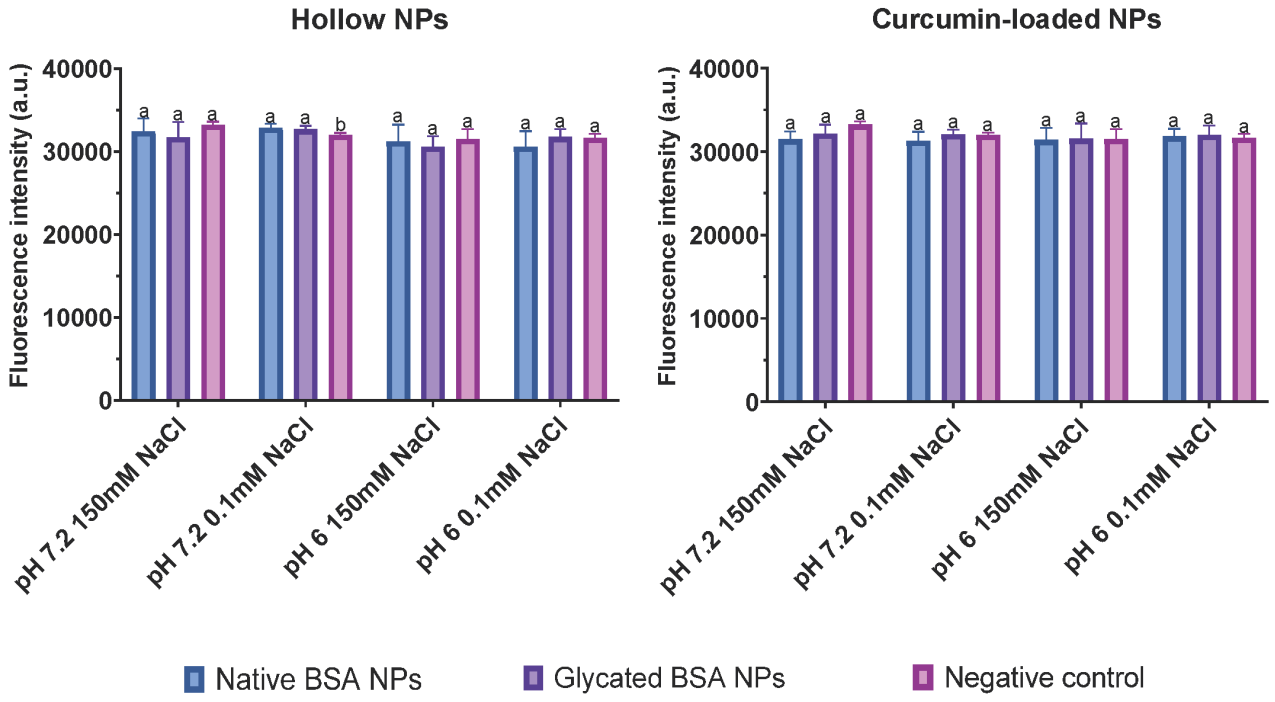

Figure 3.12 FITC-WGA fluorescence intensity.

Graph depicts FITC-WGA fluorescence intensity in the presence of hollow NPs (left) and in the presence of curcumin-loaded NPs (right). Results are grouped based on solution conditions used and means with a letter in common within the same condition group are not significantly different according to Tukey's test (where values are not significant when $P \geq 0.05$). Bars represent average value ± standard deviation (n=3, experimental replicates).

For the hollow NPs with mucin at pH 7.2 and lowest ionic strength (0.1 mM NaCl), the fluorescence intensity of FITC-WGA showed a significant increase ($P < 0.05$) compared to the negative control (Figure 3.12, left). Higher FITC fluorescence indicates more nanoparticle binding to mucin. Against their respective negative control, no other NP formulation showed increased binding to mucin and only curcumin-loaded BSA NPs showed a significant decrease ($P < 0.05$) in fluorescence intensity at pH 7.2 with 150 mM NaCl.

Different adhesive interactions are possible between mucins and nanoparticles, including hydrophobic and electrostatic interactions, and hydrogen bonding. The relative mucin-binding

property was calculated through Eq. 6. Ratios close to one reveal limited interaction between nanoparticles and mucins, compared to negative control. Mucins carry net negative charge at pHs 6.0 and 7.2, as does the negative control (BSA) because of its pI of 4.7 (Z. G. Peng et al., 2004). Figure 3.13 shows the zeta potential of hollow and curcumin-loaded NPs at the different conditions tested.

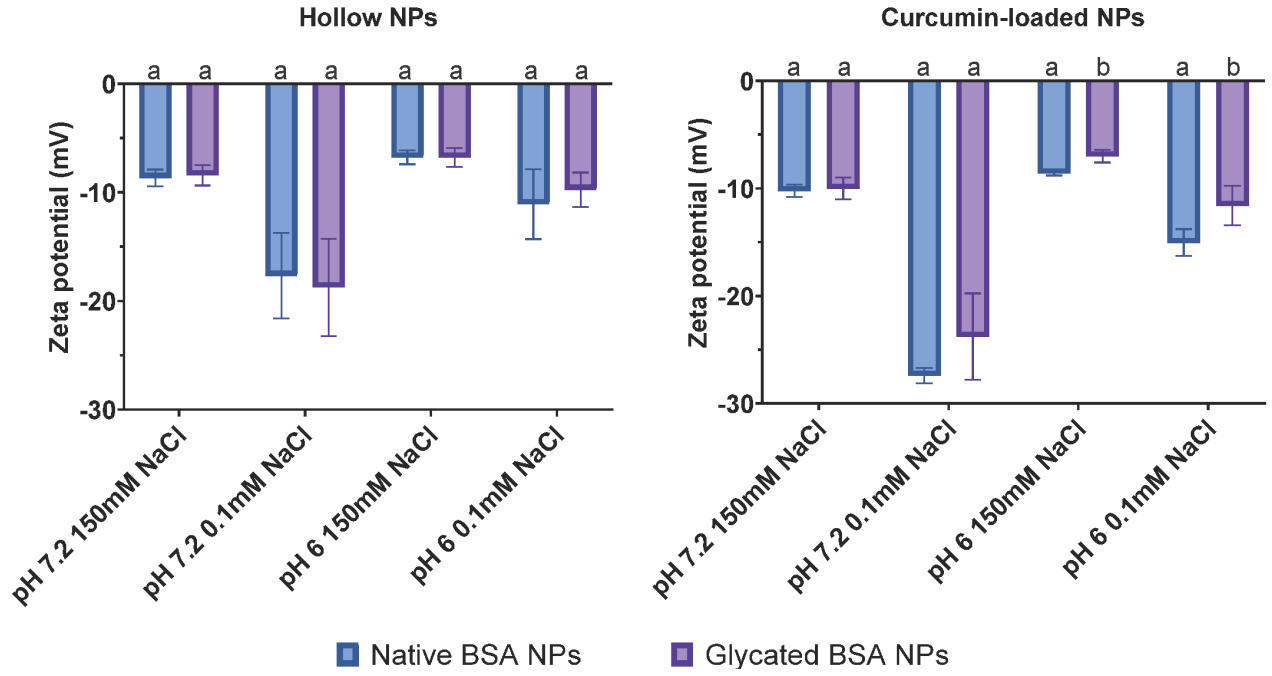

Figure 3.13 Zeta potential of nanoparticles in different conditions.

The graph on the left shows the zeta potential (mV) of hollow nanoparticles, whereas the graph on the right refers to curcumin-loaded nanoparticles. The bars represent the average value ± standard deviation (n=3, experimental replicates). Mean values with a letter in common within the same condition are not significantly different according to T-test ($P \geq 0.05$).

In Figure 3.13, NP zeta potential ranges from around -7 to -27 mV. Hollow nanoparticles (Figure 3.13, left) presented no significant difference in zeta potential when comparing glycated and native BSA NPs in the same conditions. Alternatively, a slight difference in zeta potential is

observed only when the pH is around 6.0 for the nanoparticles loaded with curcumin (Figure 3.13, right).

The negative surface charges reported in Figure 3.13 result in electrostatic repulsion towards negatively charged mucin, therefore it is logical that limited mucin-binding activity is expressed by NPs. Moreover, glycation did not result in significant difference in binding between NP and mucin. Literature indicated that *in vitro* interaction experiments with mucin are relevant and lack of binding in solution indicates absence of binding *in vivo* (Pearson et al., 2000).

Interestingly, a study with another whey protein (lactoferrin) showed strong binding between the protein and one of the major salivary mucins (MG2). The interaction of lactoferrin with MG2 caused the formation of a lactoferrin-MG2 complex *in vitro* and *in vivo* that could improve the bioactivity of lactoferrin by prolonging its presence in the oral cavity (Soares et al., 2003). Although lactoferrin was not glycated in their study, Soares et al. (2003) described the complex formation process as not dependent on the sugars in MG2's structure.

Chapter 4

Conclusions

Whey proteins have shown great potential in encapsulation and delivery of bioactive compounds, namely because of their unique properties, nutritional value and low cost (Pellegrino et al., 2013; Smithers, 2008). BSA is a suitable material for nanodelivery as its conformation adapts to ligands without losing stability and it has affinity towards hydrophobic and hydrophilic compounds (Lohcharoenkal et al., 2014; Peters, 1985). In that context, the use of BSA for encapsulation of chemically instable bioactive compounds like curcumin is valuable. Nonetheless, protecting curcumin from degradation is not sufficient to ensure good bioavailability. Mucins regulate intestinal intake of particles through selective interaction (Dekker et al., 2000) thus using it as a model to investigate bio-nano interactions corroborates to the design and application of nanocarriers.

In this study, BSA reacted with glucose under controlled conditions yielding a glycation degree of 33 ± 6%. The chemical modification was successful in enhancing physicochemical properties of BSA, in complete accordance with the literature (Ledesma-Osuna et al., 2008). The significant reduction in available amino groups combined with the observed decrease of net surface charge indicate that glycation was effective and capable of neutralizing the positive charge of Lys residues. Another significant effect of glycation was the decrease in surface hydrophobicity due to glucose's interference with hydrophobic activity through possible steric shielding (Wong et al., 2011).

The increase in static quenching indicated that more bonds were made with curcumin after glycation, even though less curcumin molecules were bound to the conjugate compared to native BSA. Not only more bonds were made in the BSA-glucose conjugate, but they were also stronger

than in the native counterpart, as indicated by the very significant increase in the Stern-Volmer quenching constant. Additionally, internalization of core Trp residues is a result of conformational changes triggered by glycation. The fluorescence quenching results revealed that the interactions with curcumin are not exclusively of hydrophobic nature and hydrogen bonds are likely responsible for the binding. Thus, the hypothesis that protein-curcumin interactions would be affected but not impaired by glycation can be accepted.

Although zeta potential changes were very significant between BSA in native conformation and the glycated counterpart, the effect of glycation on NP net surface charge was not significant. The negative surface charges of the NPs led to electrostatic repulsion towards mucin, which is also negatively charged. Glycation posed no significant impact on NP-mucin interactions compared to their respective control. Limited mucin-binding activity was expressed by all NPs regardless of surface modification, curcumin load and media conditions.

Even though no observable changes were seen in mucin-NP interactions upon glycation, there are other components and physicochemical aspects of the mucus layer that can play a role in NP adhesion and subsequent intake by epithelial cells. Mimicking biological conditions has its challenges and there is still much advancement to be done in the interpretation of *in vitro* results as *in vivo* outcomes. In the meantime, mucin is a forthcoming model for the elaboration of nano-bio interaction assays, which adds value to the design of novel nanocarriers. Differently from our results, lactoferrin formed a complex with salivary mucin *in vitro* and *in vivo* (Soares et al., 2003). As lactoferrin is also a whey protein, further investigation on mucin-NP interactions taking into consideration different types of mucin and other physiological conditions is highly encouraged.

Supplementary information

Table S.1 Estimated protein percentage in glycated BSA.

	Protein content (%)
Glycated BSA	77 ± 4

Bibliography

Albani, J. R. (2007). *Principles and applications of fluorescence spectroscopy*. Blackwell Science.

Alizadeh-Pasdar, N., & Li-Chan, E. C. Y. (2000). Comparison of protein surface hydrophobicity measured at various pH values using three different fluorescent probes. *Journal of Agricultural and Food Chemistry*, *48*(2), 328–334. https://doi.org/10.1021/jf990393p

Allen, A., & Pearson, J. P. (2000). The Gastrointestinal Adherent Mucous Gel Barrier. In A. Corfield (Ed.), *Glycoprotein Methods and Protocols: The Mucins* (Vol. 125, pp. 57–64). Humana Press.

Anand, P., Kunnumakkara, A. B., Newman, R. A., & Aggarwal, B. B. (2007). Bioavailability of curcumin: Problems and promises. In *Molecular Pharmaceutics* (Vol. 4, Issue 6, pp. 807–818). https://doi.org/10.1021/mp700113r

Arroyo-Maya, I. J., Rodiles-López, J. O., Cornejo-Mazón, M., Gutiérrez-López, G. F., Hernández-Arana, A., Toledo-Núñez, C., Barbosa-Cánovas, G. v., Flores-Flores, J. O., & Hernández-Sánchez, H. (2012). Effect of different treatments on the ability of α-lactalbumin to form nanoparticles. *Journal of Dairy Science*, *95*(11), 6204–6214. https://doi.org/10.3168/jds.2011-5103

Bezkorovainy, A. (1977). Human Milk and Colostrum Proteins: A Review. *Journal of Dairy Science*, *60*(7), 1023–1037. https://doi.org/10.3168/jds.S0022-0302(77)83984-2

Bourassa, P., Bariyanga, J., & Tajmir-Riahi, H. A. (2013). Binding sites of resveratrol, genistein, and curcumin with milk α- And β-caseins. *Journal of Physical Chemistry B*, *117*(5), 1287–1295. https://doi.org/10.1021/jp3114557

Bromberg, L. E., & Barr, D. P. (2000). Self-association of mucin. *Biomacromolecules*, *1*(3), 325–334. https://doi.org/10.1021/bm005532m

Caira, S., Pizzano, R., Picariello, G., Pinto, G., Cuollo, M., Chianese, L., & Addeo, F. (2012). Allergenicity of Milk Proteins. In *Milk Protein*. InTech. https://doi.org/10.5772/52086

Carter, D. C., & Ho, J. X. (1994). Structure of Serum Albumin. In C. B. Anfinsen, J. T. Edsall, F. M. Richards, & D. S. Eisenberg (Eds.), *Advances in Protein Chemistry* (Vol. 45, Issue C, pp. 153-undefined). https://doi.org/10.1016/S0065-3233(08)60640-3

Cas, M. D., & Ghidoni, R. (2019). Dietary curcumin: Correlation between bioavailability and health potential. *Nutrients*, *11*(9), 1–14. https://doi.org/10.3390/nu11092147

Chen, W., Lv, R., Wang, W., Ma, X., Muhammad, A. I., Guo, M., Ye, X., & Liu, D. (2019). Time effect on structural and functional properties of whey protein isolate-gum acacia conjugates prepared via Maillard reaction. *Journal of the Science of Food and Agriculture*, *99*(10), 4801–4807. https://doi.org/10.1002/jsfa.9735

Chen, W., Ma, X., Wang, W., Lv, R., Guo, M., Ding, T., Ye, X., Miao, S., & Liu, D. (2019). Preparation of modified whey protein isolate with gum acacia by ultrasound maillard reaction. *Food Hydrocolloids*, *95*, 298–307. https://doi.org/10.1016/j.foodhyd.2018.10.030

Chevalier, F., Chobert, J. M., Genot, C., & Haertlé, T. (2001). Scavenging of free radicals, antimicrobial, and cytotoxic activities of the Maillard reaction products of β-lactoglobulin glycated with several sugars. *Journal of Agricultural and Food Chemistry*, *49*(10), 5031–5038. https://doi.org/10.1021/jf010549x

Chevalier, F., Chobert, J.-M., Popineau, Y., Nicolas, M. G., & Haertle, T. (2001). Improvement of functional properties of b-lactoglobulin glycated through the Maillard reaction is related to the nature of the sugar. *International Dairy Journal*, *11*, 145–152. https://doi.org/https://doi.org/10.1016/S0958-6946(01)00040-1

Contini, C., Schneemilch, M., Gaisford, S., & Quirke, N. (2018). Nanoparticle–membrane interactions. *Journal of Experimental Nanoscience*, *13*(1), 62–81. https://doi.org/10.1080/17458080.2017.1413253

Corfield, A. P. (Ed.). (2000). *Glycoprotein Methods and Protocols: The Mucins* (Vol. 125). Humana Press.

Davidov-Pardo, G., Joye, I. J., & McClements, D. J. (2015). Food-Grade Protein-Based Nanoparticles and Microparticles for Bioactive Delivery. In *Advances in Protein Chemistry and Structural Biology* (Vol. 98, pp. 293–325). https://doi.org/10.1016/bs.apcsb.2014.11.004

Dekker, J., Jan-Willem Van Klinken, B., Büller, H. A., & Einerhand, A. W. C. (2000). Quantitation of Biosynthesis and Secretion of Mucin Using Metabolic Labeling. In A. Corfield (Ed.), *Glycoprotein Methods and Protocols: The Mucins* (Vol. 125, pp. 65–76). Humana Press.

Delaney, R. . A. . M. ., Donnelly, J. . K. ., & O'Sullivan, A. . C. . (1972). Manufacture of Undenatured Whey Protein Concentrates by Ultrafiltration and Spray Drying : 1 . Low-Protein Powders. *Irish Journal of Agricultural Research*, *11*(2), 181–192.

Elzoghby, A. O., Samy, W. M., & Elgindy, N. A. (2012). Protein-based nanocarriers as promising drug and gene delivery systems. *Journal of Controlled Release*, *161*(1), 38–49. https://doi.org/10.1016/j.jconrel.2012.04.036

Ervin, J., Sabelko, J., & Gruebele, M. (2000). Submicrosecond real-time fluorescence sampling: application to protein folding. In *J. Photochem. Photobiol. B: Biol* (Vol. 54). www.elsevier.nl/locate/jphotobiol

Fallingborg, J. (1999). Intraluminal pH of the human gastrointestinal tract. *Danish Medical Bulletin*, *43*(3), 183–196.

Fan, Y., Yi, J., Zhang, Y., Wen, Z., & Zhao, L. (2017). Physicochemical stability and in vitro bioaccessibility of β-carotene nanoemulsions stabilized with whey protein-dextran conjugates. *Food Hydrocolloids*, *63*, 256–264. https://doi.org/10.1016/j.foodhyd.2016.09.008

Fan, Y., Yi, J., Zhang, Y., & Yokoyama, W. (2018). Fabrication of curcumin-loaded bovine serum albumin (BSA)-dextran nanoparticles and the cellular antioxidant activity. *Food Chemistry*, *239*, 1210–1218. https://doi.org/10.1016/j.foodchem.2017.07.075

Farooq, M. A., Aquib, M., Ghayas, S., Bushra, R., Haleem Khan, D., Parveen, A., & Wang, B. (2019). Whey protein: A functional and promising material for drug delivery systems recent developments and future prospects. *Polymers for Advanced Technologies*, *30*(9), 2183–2191. https://doi.org/10.1002/pat.4676

Farrell, H. M., Jimenez-Flores, R., Bleck, G. T., Brown, E. M., Butler, J. E., Creamer, L. K., Hicks, C. L., Hollar, C. M., Ng-Kwai-Hang, K. F., & Swaisgood, H. E. (2004). Nomenclature of the Proteins of Cow's Milk: Sixth Revision. *Journal of Dairy Science*, *87*(6), 1641–1674. https://doi.org/10.3168/jds.S0022-0302(04)73319-6

Foegeding, E. A., Davis, J. P., Doucet, D., & McGuffey, M. K. (2002). Advances in modifying and understanding whey protein functionality. *Trends in Food Science and Technology*, *13*(5), 151–159. https://doi.org/10.1016/S0924-2244(02)00111-5

Foegeding, E., & Luck, P. (2002). Whey protein products. *Milk Proteins/Whey Protein Products*, 1957–1960. http://www.google.com/patents/US6383551

Gazme, B., Rezaei, K., & Udenigwe, C. C. (2020). Effect of enzyme immobilization and: In vitro digestion on the immune-reactivity and sequence of IgE epitopes in egg white proteins. *Food and Function*, *11*(7), 6632–6642. https://doi.org/10.1039/d0fo00938e

Gunasekaran, S., Ko, S., & Xiao, L. (2007). Use of whey proteins for encapsulation and controlled delivery applications. *Journal of Food Engineering*, *83*(1), 31–40. https://doi.org/10.1016/j.jfoodeng.2006.11.001

Guo, M., & Wang, G. (2016). Whey protein polymerisation and its applications in environmentally safe adhesives. *International Journal of Dairy Technology*, *69*(4), 481–488. https://doi.org/10.1111/1471-0307.12303

Hao, H., Ma, Q., He, F., & Yao, P. (2014). Doxorubicin and Fe3O4 loaded albumin nanoparticles with folic acid modified dextran surface for tumor diagnosis and therapy. *Journal of Materials Chemistry B*, *2*(45), 7978–7987. https://doi.org/10.1039/c4tb01359j

Hoffman, J. R., & Falvo, M. J. (2004). Protein – Which is best? *Journal of Sports Science and Medicine*, *2004*, 118–130.

Hosseini, S. M. H., Emam-Djomeh, Z., Sabatino, P., & van der Meeren, P. (2015). Nanocomplexes arising from protein-polysaccharide electrostatic interaction as a promising carrier for nutraceutical compounds. *Food Hydrocolloids*, *50*, 16–26. https://doi.org/10.1016/j.foodhyd.2015.04.006

Hounsell, E. F. (Ed.). (1993). *Glycoprotein Analysis in Biomedicine* (Vol. 14). Humana Press.

Huet, G., Delannoy, P., Lesuffleur, T., Hennebicq, S., & Degand, P. (2000). Inhibition of Mucin Glycosylation. In A. Corfield (Ed.), *Glycoprotein Methods and Protocols: The Mucins* (Vol. 125, pp. 261–272). Humana Press.

Jahanshahi, M., & Babaei, Z. (2008). Protein nanoparticle: A unique system as drug delivery vehicles. *African Journal of Biotechnology*. https://doi.org/10.5897/AJB08.081

Jayaprakasha, G. K., Chidambara Murthy, K. N., & Patil, B. S. (2016). Enhanced colon cancer chemoprevention of curcumin by nanoencapsulation with whey protein. *European Journal of Pharmacology*, *789*, 291–300. https://doi.org/10.1016/j.ejphar.2016.07.017

Jithan, A., Madhavi, K., Madhavi, M., & Prabhakar, K. (2011). Preparation and characterization of albumin nanoparticles encapsulating curcumin intended for the treatment of breast cancer. *International Journal of Pharmaceutical Investigation*, *1*(2), 119. https://doi.org/10.4103/2230-973x.82432

Jung, S. H., Choi, S. J., Kim, H. J., & Moon, T. W. (2006). Molecular characteristics of bovine serum albumin-dextran conjugates. *Bioscience, Biotechnology and Biochemistry*, *70*(9), 2064–2070. https://doi.org/10.1271/bbb.60026

Kanakis, C. D., Tarantilis, P. A., Polissiou, M. G., & Tajmir-Riahi, H. A. (2013). Probing the binding sites of resveratrol, genistein, and curcumin with milk β -lactoglobulin. *Journal of Biomolecular Structure and Dynamics*, *31*(12), 1455–1466. https://doi.org/10.1080/07391102.2012.742461

Kato, A. (2002). Industrial Applications of Maillard-Type Protein-Polysaccharide Conjugates. *Food Sci. Technol. Res*, *8*(3), 193–199.

Khanvilkar, K., Donovan, M. D., & Flanagan, D. R. (2001). Drug transfer through mucus. In *Advanced Drug Delivery Reviews* (Vol. 48). www.elsevier.com/locate/drugdeliv

Khezri S., Seyedsaleh M.M., Seyedsaleh I., Dastras M., Dehghan P. (2016). Whey: characteristics, applications and health aspects. *3rd International Conference on Science and Engineering*, *December*, 1–9. www.3icesconf.com

Khutoryanskiy, V. v. (2018). Beyond PEGylation: Alternative surface-modification of nanoparticles with mucus-inert biomaterials. In *Advanced Drug Delivery Reviews* (Vol. 124, pp. 140–149). Elsevier B.V. https://doi.org/10.1016/j.addr.2017.07.015

Kim, D. Y., & Shin, W. S. (2015). Characterisation of bovine serum albumin-fucoidan conjugates prepared via the Maillard reaction. *Food Chemistry*, *173*, 1–6. https://doi.org/10.1016/j.foodchem.2014.09.167

Kinsella, J. M., Jimenez, R. E., Karmali, P. P., Rush, A. M., Kotamraju, V. R., Gianneschi, N. C., Ruoslahti, E., Stupack, D., & Sailor, M. J. (2011). X-ray computed tomography imaging of breast cancer by using targeted peptide-labeled bismuth sulfide nanoparticles. *Angewandte Chemie - International Edition*, *50*(51), 12308–12311. https://doi.org/10.1002/anie.201104507

Kratz, F. (2008). Albumin as a drug carrier: Design of prodrugs, drug conjugates and nanoparticles. *Journal of Controlled Release*, *132*(3), 171–183. https://doi.org/10.1016/j.jconrel.2008.05.010

Laemmli, U. K. (1970). Cleavage of Structural Proteins during the Assembly of the Head of Bacteriophage T4. *Nature*, *227*, 680–685. https://doi.org/https://doi.org/10.1038/227680a0

Ledesma-Osuna, A. I., Ramos-Clamont, G., & Vázquez-Moreno, L. (2008). Characterization of bovine serum albumin glycated with glucose, galactose and lactose. *Acta Biochimica Polonica*, *55*(3), 491–497. https://doi.org/10.18388/abp.2008_3054

Leroueil, P. R., Hong, S., Mecke, A., Jr, J. R. B., Orr, G., & Holl, M. M. B. (2008). *Nanoparticle Interaction with Biological Membranes*. *40*(5), 335–342. https://doi.org/10.1021/ar600012y.Nanoparticle

Lesniak, A., Salvati, A., Santos-Martinez, M. J., Radomski, M. W., Dawson, K. A., & Åberg, C. (2013). Nanoparticle adhesion to the cell membrane and its effect on nanoparticle uptake efficiency. *Journal of the American Chemical Society*, *135*(4), 1438–1444. https://doi.org/10.1021/ja309812z

Liang, L., Tajmir-Riahi, H. A., & Subirade, M. (2008). Interaction of β-Lactoglobulin with resveratrol and its biological implications. *Biomacromolecules*, *9*(1), 50–56. https://doi.org/10.1021/bm700728k

Lin, J. A., Wu, C. H., & Yen, G. C. (2018). Perspective of Advanced Glycation End Products on Human Health. *Journal of Agricultural and Food Chemistry*, *66*(9), 2065–2070. https://doi.org/10.1021/acs.jafc.7b05943

Liu, G., & Zhong, Q. (2012). Glycation of whey protein to provide steric hindrance against thermal aggregation. *Journal of Agricultural and Food Chemistry*, *60*(38), 9754–9762. https://doi.org/10.1021/jf302883b

Liu, G., & Zhong, Q. (2013). Thermal aggregation properties of whey protein glycated with various saccharides. *Food Hydrocolloids*, *32*, 87–96.

Liu, J., & Jing, H. (2016). Glycation of bovine serum albumin with monosaccharides inhibits heat-induced protein aggregation. *RSC Advances*, *6*(116), 115183–115188. https://doi.org/10.1039/c6ra24580c

Livney, Y. D. (2010). Milk proteins as vehicles for bioactives. In *Current Opinion in Colloid and Interface Science* (Vol. 15, Issues 1–2, pp. 73–83). https://doi.org/10.1016/j.cocis.2009.11.002

Lohcharoenkal, W., Wang, L., Charlie Chen, Y., & Rojanasakul, Y. (2014). Protein nanoparticles as drug delivery carriers for cancer therapy. *BioMed Research International*, *4*, 1–12.

Lund, M. N., & Ray, C. A. (2017). Control of Maillard Reactions in Foods: Strategies and Chemical Mechanisms. *Journal of Agricultural and Food Chemistry*, *65*(23), 4537–4552. https://doi.org/10.1021/acs.jafc.7b00882

Majorek, K. A., Porebski, P. J., Dayal, A., Zimmerman, M. D., Jablonska, K., Stewart, A. J., Chruszcz, M., & Minor, W. (2012). Structural and immunologic characterization of bovine, horse, and rabbit serum albumins. *Molecular Immunology*, *52*(3–4), 174–182. https://doi.org/10.1016/j.molimm.2012.05.011

Marshall, K. (2004). Therapeutic applications of whey protein. *Alternative Medicine Review*, *9*(2), 136–156.

Matulis, D., & Lovrien, R. (1998). *-Anilino-8-Naphthalene Sulfonate Anion-Protein Binding Depends Primarily on Ion Pair Formation*.

Mehravar, R., Jahanshahi, M., & Saghatoleslami, N. (2009). Production of biological nanoparticles from α-lactalbumin for drug delivery and food science application. *African Journal of Biotechnology*, *8*(24), 6822–6827. https://doi.org/10.5897/AJB2009.000-9530

Mohammadi, F., Bordbar, A. K., Mohammadi, K., Divsalar, A., & Saboury, A. A. (2010). Circular dichroism and fluorescence spectroscopic study on the interaction of bisdemethoxycurcumin and diacetylbisdemethoxycurcumin with human serum albumin. *Canadian Journal of Chemistry*, *88*(2), 155–163. https://doi.org/10.1139/V09-169

Mohammadian, M., Salami, M., Momen, S., Alavi, F., Emam-Djomeh, Z., & Moosavi-Movahedi, A. A. (2019). Enhancing the aqueous solubility of curcumin at acidic condition through the complexation with whey protein nanofibrils. *Food Hydrocolloids*, *87*(September 2018), 902–914. https://doi.org/10.1016/j.foodhyd.2018.09.001

Morgan, F., Léonil, J., Mollé, D., & Bouhallab, S. (1999). Modification of bovine β-lactoglobulin by glycation in a powdered state or in an aqueous solution: Effect on association behavior and protein conformation. *Journal of Agricultural and Food Chemistry*, *47*(1), 83–91. https://doi.org/10.1021/jf9804387

Moro, A., Gatti, C., & Delorenzi, N. (2001). Hydrophobicity of whey protein concentrates measured by fluorescence quenching and its relation with surface functional properties. *Journal of Agricultural and Food Chemistry*, *49*(10), 4784–4789. https://doi.org/10.1021/jf001132e

Murthy, K. N. C., Monika, P., Jayaprakasha, G. K., & Patil, B. S. (2018). Nanoencapsulation: An advanced nanotechnological approach to enhance the biological efficacy of curcumin. *ACS Symposium Series*, *1286*, 383–405. https://doi.org/10.1021/bk-2018-1286.ch0021

Nielsen, P. M., Petersen, D., & Dambmann, C. (2001). Improved Method for Determining Food Protein Degree of Hydrolysis. In *Food Chemistry and Toxicology JFS: Food Chemistry and Toxicology* (Vol. 66, Issue 5).

Noguchi, Y., Wu, J., Duncan, R., Strohalm, J., Ulbrich, K., Akaike, T., & Maeda, H. (1998). Early phase tumor accumulation of Macromolecules: A great difference in clearance rate between tumor and normal tissues. *Japanese Journal of Cancer Research*, *89*(3), 307–314. https://doi.org/10.1111/j.1349-7006.1998.tb00563.x

Nosrati, H., Sefidi, N., Sharafi, A., Danafar, H., & Kheiri Manjili, H. (2018). Bovine Serum Albumin (BSA) coated iron oxide magnetic nanoparticles as biocompatible carriers for curcumin-anticancer drug. *Bioorganic Chemistry*, *76*, 501–509.

Okagu, O. D., Jin, J., & Udenigwe, C. C. (2021). Impact of succinylation on pea protein-curcumin interaction, polyelectrolyte complexation with chitosan, and gastrointestinal release of

curcumin in loaded-biopolymer nano-complexes. *Journal of Molecular Liquids*, *325*. https://doi.org/10.1016/j.molliq.2020.115248

Okagu, O. D., Verma, O., McClements, D. J., & Udenigwe, C. C. (2020). Utilization of insect proteins to formulate nutraceutical delivery systems: Encapsulation and release of curcumin using mealworm protein-chitosan nano-complexes. *International Journal of Biological Macromolecules*, *151*, 333–343. https://doi.org/10.1016/j.ijbiomac.2020.02.198

O'Mahony, J. A., & Fox, P. F. (2013). Milk Proteins: Introduction and Historical Aspects. In P. L. H. McSweeney & P. F. Fox (Eds.), *Advanced Dairy Chemistry - Volume 1A: Proteins: Basic Aspects* (4th ed., pp. 43–85). Springer US. https://doi.org/10.1007/978-1-4614-4714-6

Pan, Y., Li, X. M., Meng, R., & Zhang, B. (2020). Exploration of the Stabilization Mechanism and Curcumin Bioaccessibility of Emulsions Stabilized by Whey Protein Hydrolysates after Succinylation and Glycation in Different Orders [Research-article]. *Journal of Agricultural and Food Chemistry*, *68*(2), 623–632. https://doi.org/10.1021/acs.jafc.9b07350

Pan, Y., Wu, Z., Xie, Q. T., Li, X. M., Meng, R., Zhang, B., & Jin, Z. Y. (2020). Insight into the stabilization mechanism of emulsions stabilized by Maillard conjugates: Protein hydrolysates-dextrin with different degree of polymerization. *Food Hydrocolloids*, *99*(August 2019), 105347. https://doi.org/10.1016/j.foodhyd.2019.105347

Patel, S. (2015). Functional food relevance of whey protein: A review of recent findings and scopes ahead. *Journal of Functional Foods*, *19*, 308–319. https://doi.org/10.1016/j.jff.2015.09.040

Pearson, J. P., Allen, A., & Hutton, D. A. (2000). Rheology of Mucin. In A. Corfield (Ed.), *Glycoprotein Methods and Protocols: The Mucins* (Vol. 125, pp. 99–112). Humana Press.

Pellegrino, L., Masotti, F., Cattaneo, S., Hogenboom, J. A., & Noni, I. de. (2013). Nutritional Quality of Milk Proteins. In P. L. H. McSweeney & P. F. Fox (Eds.), *Advanced Dairy*

Chemistry - Volume 1A: Proteins: Basic Aspects (4th ed., pp. 515–538). Springer US. https://doi.org/10.1007/978-1-4614-4714-6

Peng, H., Gan, Z., Xiong, H., Luo, M., Yu, N., Wen, T., Wang, R., & Li, Y. (2017). Self-Assembly of Protein Nanoparticles from Rice Bran Waste and Their Use as Delivery System for Curcumin. *ACS Sustainable Chemistry and Engineering*, *5*(8), 6605–6614. https://doi.org/10.1021/acssuschemeng.7b00851

Peng, Z. G., Hidajat, K., & Uddin, M. S. (2004). Adsorption of bovine serum albumin on nanosized magnetic particles. *Journal of Colloid and Interface Science*, *271*(2), 277–283. https://doi.org/10.1016/j.jcis.2003.12.022

Peters, T. (1985). Serum Albumin. *Advances in Protein Chemistry*, *37*(C), 161–245. https://doi.org/10.1016/S0065-3233(08)60065-0

Prajitha, N., Athira, S. S., & Mohanan, P. v. (2019). Bio-interactions and risks of engineered nanoparticles. *Environmental Research*, *January*, 98–108. https://doi.org/10.1016/j.envres.2019.02.003

Rafiee, Z., Nejatian, M., Daeihamed, M., & Jafari, S. M. (2019). Application of different nanocarriers for encapsulation of curcumin. *Critical Reviews in Food Science and Nutrition*, *59*(21), 3468–3497. https://doi.org/10.1080/10408398.2018.1495174

Ramos, O. L., Pereira, R. N., Simões, L. S., Madalena, D. A., Rodrigues, R. M., Teixeira, J. A., & Vicente, A. A. (2019). Nanostructures of whey proteins for encapsulation of food ingredients. In *Biopolymer Nanostructures for Food Encapsulation Purposes*. https://doi.org/10.1016/b978-0-12-815663-6.00003-3

Rondeau, P., Armenta, S., Caillens, H., Chesne, S., & Bourdon, E. (2007). Assessment of temperature effects on b-aggregation of native and glycated albumin by FTIR spectroscopy

and PAGE: Relatins between structural changes and antioxidant properties. *Archives of Biochemistry and Biophysics*, *460*, 141–150.

Rondeau, P., Navarra, G., Cacciabaudo, F., Leone, M., Bourdon, E., & Militello, V. (2010). Thermal aggregation of glycated bovine serum albumin. *Biochimica et Biophysica Acta*, *1804*, 789–798.

Salehiabar, M., Nosrati, H., Javani, E., Aliakbarzadeh, F., Kheiri Manjili, H., Davaran, S., & Danafar, H. (2018). Production of biological nanoparticles from bovine serum albumin as controlled release carrier for curcumin delivery. *International Journal of Biological Macromolecules*, *115*, 83–89. https://doi.org/10.1016/j.ijbiomac.2018.04.043

Sambrook, J., Ashwell, J., Morell, G., Ishil, A. G., Inoue, H., Chujo, Y., Maeji, R., Inoue, N. J., Mimura, R., Inoue, Y., Maeji, Y., Chujo, N. J., Veber, R., Holly, D. F., Paleveda, F. W., Nutt, W. J., Matsuura, R. F., Greene, H., & Hakomori, T. (1993). Effects of Glycosylation on Peptide Backbone. In *Ado. Ertzymol. Relat. Areas Mol. Biol* (Vol. 115, Issue 2). https://pubs.acs.org/sharingguidelines

Sanidad, K. Z., Sukamtoh, E., Xiao, H., McClements, D. J., & Zhang, G. (2019). Curcumin: Recent Advances in the Development of Strategies to Improve Oral Bioavailability. *Annual Review of Food Science and Technology*, *10*(1), 597–617. https://doi.org/10.1146/annurev-food-032818-121738

Sigurdsson, H. H., Kirch, J., & Lehr, C. M. (2013). Mucus as a barrier to lipophilic drugs. In *International Journal of Pharmaceutics* (Vol. 453, Issue 1, pp. 56–64). Elsevier B.V. https://doi.org/10.1016/j.ijpharm.2013.05.040

Singh, V. P., Bali, A., Singh, N., & Jaggi, A. S. (2014). Advanced glycation end products and diabetic complications. *Korean Journal of Physiology and Pharmacology*, *18*(1), 1–14. https://doi.org/10.4196/kjpp.2014.18.1.1

Smithers, G. W. (2008). Whey and whey proteins-From "gutter-to-gold." *International Dairy Journal*, *18*(7), 695–704. https://doi.org/10.1016/j.idairyj.2008.03.008

Sneharani, A. H., Karakkat, J. v., Singh, S. A., & Rao, A. G. A. (2010). Interaction of curcumin with ß-lactoglobulin - stability, spectroscopic analysis, and molecular modeling of the complex. *Journal of Agricultural and Food Chemistry*, *58*(20), 11130–11139. https://doi.org/10.1021/jf102826q

Soares, R. v., Siqueira, C. C., Bruno, L. S., Oppenheim, F. G., Offner, G. D., & Troxler, R. F. (2003). MG2 and lactoferrin form a heteropic complex in salivary secretions. *Journal of Dental Research*, *82*(6), 471–475.

Sułkowska, A. (2002). Interaction of drugs with bovine and human serum albumin. *Journal of Molecular Structure*, *614*, 227–232. www.elsevier.com/locate/molstruc

Sun, C., Lee, J. S. H., Zhang, M., Fang, C., Stephen, Z., Veiseh, O., Hansen, S., Ellenbogen, R. G., Olson, J., & Zhang, M. (2008). Tumor-targeted drug delivery and MRI contrast enhancement by chlorotoxin-conjugated iron oxide nanoparticles. *Nanomedicine*, *3*(4), 495–505. https://doi.org/10.2217/17435889.3.4.495.Tumor-targeted

Taghavi Kevij, H., Mohammadian, M., & Salami, M. (2019). Complexation of curcumin with whey protein isolate for enhancing its aqueous solubility through a solvent-free pH-driven approach. *Journal of Food Processing and Preservation*, *43*(12), 1–9. https://doi.org/10.1111/jfpp.14227

Tayeh, N., Rungassamy, T., & Albani, J. R. (2009). Fluorescence spectral resolution of tryptophan residues in bovine and human serum albumins. *Journal of Pharmaceutical and Biomedical Analysis*, *50*(2), 107–116. https://doi.org/10.1016/j.jpba.2009.03.015

Teng, Z., Li, Y., & Wang, Q. (2014). Insight into curcumin-loaded β-lactoglobulin nanoparticles: Incorporation, particle disintegration, and releasing profiles. *Journal of Agricultural and Food Chemistry*, *62*(35), 8837–8847. https://doi.org/10.1021/jf503199g

Tsekovska, R., Sredovska-Bozhinov, A., Niwa, T., Ivanov, I., & Mironova, R. (2016). Maillard reaction and immunogenicity of protein therapeutics. *World Journal of Immunology*, *6*(1), 19. https://doi.org/10.5411/wji.v6.i1.19

Tunick, M. H. (2008). Whey Protein Production and Utilization: A Brief History. In C. I. Onwulata & P. J. Huth (Eds.), *Whey Processing, Functionality and Health Benefits* (pp. 17–99). Wiley-Blackwell. https://doi.org/10.1002/9780813803845

Ullrey, D. E. (2009a). Vitamins and mineral elements. In *Adequate Food for All: Culture, Science, and Technology of Food in the 21st Century* (pp. 103–126). https://doi.org/10.1201/9781420077544

Ullrey, D. E. (2009b). Protein and amino acids. In *Adequate Food for All: Culture, Science, and Technology of Food in the 21st Century* (pp. 95–101). CRC Press. https://doi.org/10.1201/9781420077544

van der Schans, C. P., & Rubin, B. K. (Eds.). (2004). *Therapy for Mucus-Clearance Disorders* (Vol. 188). Marcel Dekker, Inc.

Vivian, J. T., & Callis, P. R. (2001). Mechanisms of tryptophan fluorescence shifts in proteins. *Biophysical Journal*, *80*(5), 2093–2109. https://doi.org/10.1016/S0006-3495(01)76183-8

Wang, G., Siggers, K., Zhang, S., Jiang, H., Xu, Z., Zernicke, R. F., Matyas, J., & Uludağ, H. (2008). Preparation of BMP-2 containing bovine serum albumin (BSA) nanoparticles stabilized by polymer coating. *Pharmaceutical Research*, *25*(12), 2896–2909. https://doi.org/10.1007/s11095-008-9692-2

Wong, B. T., Day, L., & Augustin, M. A. (2011). Deamidated wheat protein-dextran Maillard conjugates: Effect of size and location of polysaccharide conjugated on steric stabilization of emulsions at acidic pH. *Food Hydrocolloids*, *25*(6), 1424–1432. https://doi.org/10.1016/j.foodhyd.2011.01.017

Wu, L., Garnett, M. C., Davies, M. C., Bignotti, F., Ferruti, P., Davis, S. S., & Illum, L. (1997). Preparation of surface-modified albumin nanospheres. *Biomaterials*, *18*(7), 559–565. https://doi.org/10.1016/S0142-9612(96)00176-7

Yang, W., Tu, Z., Wang, H., Zhang, L., & Song, Q. (2018). Glycation of ovalbumin after high-intensity ultrasound pretreatment: effects on conformation, immunoglobulin (Ig)G/IgE binding ability and antioxidant activity. *Journal of the Science of Food and Agriculture*, *98*(10), 3767–3773. https://doi.org/10.1002/jsfa.8890

Yi, J., Fan, Y., Zhang, Y., Wen, Z., Zhao, L., & Lu, Y. (2016). Glycosylated α-lactalbumin-based nanocomplex for curcumin: Physicochemical stability and DPPH-scavenging activity. *Food Hydrocolloids*, *61*, 369–377. https://doi.org/10.1016/j.foodhyd.2016.05.036

Yi, J., Lam, T. I., Yokoyama, W., Cheng, L. W., & Zhong, F. (2014). Controlled release of β-carotene in β-lactoglobulin-dextran- conjugated nanoparticles" in vitro digestion and transport with caco-2 monolayers. *Journal of Agricultural and Food Chemistry*, *62*(35), 8900–8907. https://doi.org/10.1021/jf502639k

Zhang, Q., Li, L., Lan, Q., Li, M., Wu, D., Chen, H., Liu, Y., Lin, D., Qin, W., Zhang, Z., Liu, J., & Yang, W. (2019). Protein glycosylation: a promising way to modify the functional properties and extend the application in food system. *Critical Reviews in Food Science and Nutrition*, *59*(15), 2506–2533. https://doi.org/10.1080/10408398.2018.1507995